TAMPEREEN TEKNILLINEN YLIOPISTO
TAMPERE UNIVERSITY OF TECHNOLOGY

ANTTI AHO

EXPERIMENTAL STUDY ON ADSORPTION STORAGE OF GASES ON SOLID MATERIALS

Master of Science Thesis

Examiners: Professor Risto Raiko
and M.Sc. Henrik Tolvanen
Examiners and topic approved at the
Faculty of Science and
Environmental Engineering Council
meeting on 5.11.2014

ABSTRACT

TAMPERE UNIVERSITY OF TECHNOLOGY
Master's Degree Programme in Environmental and Energy Engineering
AHO, ANTTI: Experimental study on adsorption storage of gases on solid materials
Master of Science Thesis, 56 pages, no Appendix pages
March 2015
Major: Power Plant and Combustion Technology
Examiners: Professor Risto Raiko and M.Sc. Henrik Tolvanen
Keywords: Natural gas storage, gas adsorption, ANG

The goal of this thesis was to study adsorption storage of gases, mainly methane, in porous solids. The study included reviewing literature, building an experimental setup, preparation of samples, adsorption measurements and the analysis of the results.

An experimental setup was constructed to study the bulk storage of gases. The setup was based on the gravimetric method, but due to limitations in both funding and time, the accuracy of the setup is far from that of its commercial equivalents. It, however, enables the studying of bulk storage properties of large sample amounts, which allows the elimination of uncertainty due to sample heterogeneity. A minimum sample amount of 50 g is recommended for future experiments.

Carbon samples were prepared to be studied as adsorbents. Spruce cubes were carbonized with both slow and high heating rate and some of the samples were chemically activated to produce activated carbon. Adsorption on a commercial activated carbon was studied for comparison. Uptake values of approximately 0.05 $\pm$ 0.02 g_{CH4}/g_{carbon} in 35 bar and 22 °C were measured for both the best prepared activated carbon sample and the commercial carbon sample. The uptake is much lower than the uptake goal set by the U.S. Department of Energy of 0.5 g_{CH4}/g_{carbon}, which shows the difficulty of preparing of good adsorbents.

TIIVISTELMÄ

TAMPEREEN TEKNILLINEN YLIOPISTO
Ympäristö- ja energiatekniikan koulutusohjelma
AHO, ANTTI: Kokeellinen tutkimus kaasujen adsorptiovarastoinnista
Diplomityö, 56 sivua, ei liitesivuja
Maasliskuu 2015
Pääaine: Voimalaitos- ja polttotekniikka
Tarkastajat: Professori Risto Raiko, DI Henrik Tolvanen
Avainsanat: Metaanin varastointi, kaasujen adsorptio, ANG

Tämän työn tavoitteena oli tutkia kaasujen, pääasiassa metaanin, adsorptiovarastointia huokoisiin materiaaleihin. Työhön sisältyy alan kirjallisuuden selvitystä, kokeellisen laitteiston rakentaminen, näytteiden valmistusta, adsorptiomittauksia ja tulosten analysointia.

Koelaitteisto rakennettiin tutkimaan kaasujen adsorptiovarastointia. Koelaitteisto perustuu näytteen ja kaasun punnitukseen, mutta kärsii huomattavasta epätarkkuudesta pienillä näytemäärillä johtuen laitteiston suunnittelusta, rahoituksellisista sekä ajankäytöllisistä ongelmista. Tulevissa mittauksissa suositellaan käyttämään vähintään 50 g:n näytemäärää.

Kuusipuusta valmistettiin lämpökäsittelyllä hiiltä, jota käytettiin adsorptiomittauksissa. Näytteitä tuotettiin niin hitaalla kuin nopealla lämmönnostonopeudella, osa näytteistä koki vain lämpökäsittelyn ja osa aktivoitiin kemiallisesti. Mittauksia tehtiin myös kaupalliselle aktiivihiilelle. Mittauksissa parhaalle valmistetulle aktiivihiilelle saatiin varastointitiheydeksi 0.05 ± 0.02 g_{CH4}/g_{hiili} kun paine oli 35 bar(a) ja lämpötila 22 °C, mikä on hyvin pieni verrattuna USA:n energiaministeriön asettamaan tavoitteeseen 0.5 g_{CH4}/g_{hiili}. Tämä osoittaa, että hyvien adsorptiomateriaalien valmistus on hyvin haastavaa.

PREFACE

This work was carried out at the Tampere University of Technology on the department of Chemistry and Bioengineering, starting in June 2014 and finished in March 2015. I would like to thank Professor Risto Raiko for providing me with the chance to work on this thesis and for his aid and insight through the project.

My gratitude also goes to M.Sc. Henrik Tolvanen for guiding the work and for his help in both the experimental and theoretical part.

The help and knowledge of Jarmo Ruusila was invaluable during the construction of the setup.

Finally, my gratitude and my thanks go to my life partner for her love and support during the work.

Tampere, March 2015

Antti Aho

CONTENTS

ABBREVIATIONS AND NOTATION

Symbols	Units	Definition
A	-	Peng-Robinson equation coefficient
A	J $Å^{12}$	Lennard-Jones constant
A	m^2	area of one molecule
a	kg $m^5 mol^{-2}$ s^{-2}	Peng-Robinson equation coefficient
B	-	Peng-Robinson equation coefficient
B	J $Å^6$	Lennard-Jones constant
b	$m^3 mol^{-1}$	Peng-Robinson equation coefficient
C	-	Relative lifetime of adsorbed molecules
E	V m^{-1}	electric field
k	-	Freundlich isotherm constant
k	-	Langmuir isotherm constant
M	kg mol^{-1}	molar mass
m	kg	mass
n	-	Freundlich isotherm constant
p	Pa	pressure
Q	C m^2	field gradient-quadrupole
r	m	mercury curvature radius
r	Å	distance between particles
S	m^2/g	surface area
V	m^3	volume
X	kg	adsorbed mass
Z	-	compressibility factor
R_u	J $mol^{-1} K^{-1}$	universal gas constant, 8.314 J $mol^{-1} K^{-1}$

Greek symbols	Units	Definition
α	-	Peng-Robinson equation coefficient
α	C m^2 V^{-1}	polarizability
γ	N m^{-1}	surface tension
ϵ	J	potential well depth
θ	$^\circ$	contact angle
θ	-	Langmuir isotherm coverage
κ	-	Peng-Robinson equation coefficient
μ	C m	dipole
σ	Å	van der Waals radius
ϕ	J	potential energy
ω	-	acentric factor

Notation	**Definition**
bar(a)	bar absolute pressure
bar	bar gauge pressure
Nm3	Normal cubic metre (NTP)

Subscripts	**Definition**
0	saturation pressure
a	adsorbed, adsorption
BET	Brunauer-Emmett-Teller
c	property of a specie in the critical point
d	desorption
ex	excess adsorption
LJ	Lennard-Jones
m	bulk fluid
m	monolayer
p	polarization
Q	field gradient-quadrupole
r	reduced variable
s	sorbate
μ	field-dipole

Abbreviation	**Definition**
AC	Activated carbon
ACF	Activated carbon fiber
ANG	Adsorbed natural gas
ACM	Activated carbon monolith
BFB	Bubbling fluidized bed reactor
CNG	Compressed natural gas
GAC	Granular activated carbon
LNG	Liquefied natural gas
MOF	Metal-organic framework
NG	Natural gas
PAC	Powdered activated carbon
PSA	Pressure swing adsorption
SSA	Specific surface area

LIST OF FIGURES

LIST OF TABLES

1. INTRODUCTION

Increasing carbon dioxide (CO_2) emissions and their effect on the climate change have lately raised a great deal of attention. The use of alternative energy sources has increased, yet fossil fuels are still a major source of energy in the world [29]. Combustion of natural gas produces lower emissions than oil and coal and it could be used to replace them in many applications. Hydrogen has been named as the fuel of the future due to its high gravimetric energy content and the emissions composed only of water vapor [18].

A major problem with natural gas and hydrogen is their low volumetric energy density. Both of them may be compressed, but still reaching only fractions of the energy density of gasoline. Liquefaction and chemical storage methods can be used, but they have their limitations [12; 79]. Storing gases in porous solids based on adsorption might solve the problems with gas storage energy density [9].

The aim of this thesis is to study the adsorption storage of gases, with a focus on methane. Adsorption storage could be used both in large scale passive storage of natural gas and in vehicular fuel storage. Large amounts of gas could be stored passively, with no required energy input, in pressures commonly used in natural gas transport pipelines. This kind of storage could be used adjacent to a power plant provide supply security, allow the plant to be disconnected from the gas transport network, and to balance price changes. Adsorption storage could be utilized in carbon capture and storage (CCS) applications to store CO_2 [39; 11; 78].

Many carbonaceous waste materials, with little other use, could be used as precursors for highly porous adsorbents [31; 32]. If the price of carbon emissions is set to rise, it could make adsorbent production an attractive alternative to combustion for many materials.

In the beginning of this work the properties and the significance of natural gas are reviewed. An overview on adsorption as a phenomenom is given with examples on adsorbent materials and their characterization. The measurement setup and procedure are introduced, after which the experimental results are presented and discussed.

2. NATURAL GAS

The storage of natural gas was studied in this work by examining the adsorption storage of methane, the main component of natural gas. The storage applications for other gases are reviewed later in the work.

2.1 Properties

Natural gas (NG) is a colorless and an odorless gas. The chemical composition of natural gas varies greatly depending on the field it was recovered from, as can be seen in table 2.1, but it mainly consists of methane along with some heavier hydrocarbons.

Natural gas is usually processed at the wellhead to remove some of the higher hydrocarbons, water and other unwanted impurities such as hydrogen sulfide. However, as natural gas is highly flammable, it is typically odorized before distribution to domestic use. A strongly smelling, clearly noticeable substance such as THT or ethyl mercaptan is added to the gas so that potential gas leaks can be detected more easily [70].

Typical properties of natural gas can be seen in table 2.2.

Combustion of methane produces 30 % less CO_2 than oil and about 45 % less than coal, which makes it an interesting fuel in trying to reduce emissions. It also burns much cleaner with fewer small particles and SOx produced than other fossil fuels. NOx emissions for LNG seem to be on the same level with coal due to the liquefaction

Table 2.1: Typical chemical composition of natural gas from certain gas fields [69].

Component		The Russian Federation, Urengoi	Germany, Goldenstedt	USA, Kansas	The Netherlands, Groningen
Methane	CH_4	98 %	88.0 %	84.1 %	81.3 %
Ethane	C_2H_6	0.8 %	1.0 %	6.7 %	2.8 %
Propane	C_3H_8	0.2 %	0.2 %	0.3 %	0.4 %
Butane	C_4H_{10}	0.02 %	-	-	0.4 %
Nitrogen	N_2	0.9 %	10.0 %	8.4 %	14.3 %
Carbon dioxide	CO_2	0.1 %	0.8 %	0.8 %	0.9 %

Table 2.2: Typical properties of natural gas [69].

Property		Value	
Density (NTP)		0.65	kg/m^3
Boiling point		-161.5	°C
Critical point	temperature	-82.6	°C
	pressure	46.0	bar
Kinetic diameter		0.38	nm
Heating value	lower (LHV)	36.0	MJ/Nm^3
		50.0	MJ/kg
	gross (GHV)	39.8	MJ/Nm^3
		55.3	MJ/kg
Flammability limit	lower (LEL)	5	vol-%
	upper (UFL)	15	vol-%

and regasification [34]. However, methane is a much more potent greenhouse gas than CO_2, with the methane emissions produced by the natural gas and petroleum systems covering 29 % of the total methane emissions in the U.S [73].

2.2 Storage and transport methods

Currently natural gas can be stored and transported as either compressed natural gas (CNG) or liquefied natural gas (LNG). A comparison of the different methods can be found in table 2.3. CNG is typically transported in natural gas pipelines at pressures up to 100 bar. The pipeline itself acts as a storage and a buffer, as the volume in transport pipelines is quite large and the pressure can be temporarily increased if higher demand is expected in the near future [38]. For seasonal large scale storage, natural gas can be injected into depleted natural gas reservoirs, water aquifers or salt caverns [5].

LNG provides flexibility over pipeline delivery of natural gas. LNG can be shipped with carriers and delivered with trucks or trains where it is needed, even to places with no pipeline infrastructure. As the LNG market today is global, LNG may improve the energy supply security by lowering the dependency on a source in the case of a single gas provider, as is the case with Finland and many Eastern European countries [19]. Due to the high initial costs of building a liquefaction plant, LNG is typically not economically viable for transport distances below 1600 km for offshore or 3200 km onshore [16]. One liquefaction plant has been built in Finland and plans for LNG terminals exist, yet none have been built yet. [25; 77].

Adsorbed natural gas (ANG) has the benefit of being able to store NG in a lower pressure than CNG but in a much more stabile form than LNG. When a container is

Table 2.3: Comparison of different storage methods.

	Temperature [°C]	Pressure [bar(a)]	ρ [kg/m^3]	Relative density
Natural gas	25	1	0.65	1
CNG	25	200	150	230
LNG	-161.5	1	400	615
ANG	25	35	130	200

filled with a suitable porous solid material, more NG can be fit in it at a lower pressure than if the gas was just compressed in an empty container. As the pressure is lower, lighter containers can be used which also enables the construction of different shaped containers than the cylinders used for CNG, making ANG easier to use for vehicular applications [12]. Lower pressures also directly translate to better safety in traffic accident situations ANG has also been proposed for use in large scale gas storage [45; 61].

Two different terms are commonly used to describe the adsorption potential of a material: storage and delivery. Storage describes how much gas can be stored in the material, and delivery describes how much gas can be released when the pressure is lowered from storage pressure to ambient pressure. These two values usually differ slightly, with delivery typically being lower. The difference corresponds to the gas that is still adsorbed in the material and that cannot be removed in ambient conditions without heating the storage. A certain pressure level is needed so that the gas can be fed to the engine at a high enough rate. The actual usable volume might be even lower than the definded delivery value because of this.

2.3 Use

Global natural gas demand in 2013 was 3.35 trillion cubic meters, and it is estimated to rise to 3.4 trillion cubic meters by 2015 [6; 30]. Natural gas covers approximately 15 % of the total energy consumption of the world [29] and 7.8 % of Finland's total energy consumption [72].

The use of natural gas as a transportation fuel has grown strongly, yet it still only covers 0.7 % of the gas usage in the world. In some countries like Iran and Pakistan the number of NG vehicles is over 50 % of the total vehicle population, but in those countries NG covers less than 20 % of the total fuel consumption. In Bangladesh and Armenia the natural gas consumption in vehicular use is above 50 % [52; 54; 53]. Marine use of LNG has some potential in replacing currently used bunker fuel due to the increasing emission restrictions of ships. Using natural and forced boil-off gases for propulsion in LNG carriers could bring major savings [17].

The Department of Energy of the United States has set a goal for vehicular ANG storage capacity of 180 v/v, and lately increased this goal to 263 v/v STP (273.15 K, 1 atm) [15]. This means a storage capacity of 263 cm^3 of NG in one cubic centimeter of storage. Gravimetric density should be 0.5 g of NG in one gram of sorbent, and the cost of the sorbent should be below $10/kg.

Natural gas is a fossil fuel and is not usually considered as a 'clean energy' solution. However, it has been proposed by some authors that natural gas could be used as a carbon neutral source for hydrogen with the help of catalytic decomposition of methane [10; 20]. As the reaction produces gaseous hydrogen and solid carbon, the removal of carbon could be much easier and economically more viable than the removal of the carbon dioxide after the combustion from the flue gases.

2.4 Global reserves

Natural gas can be found conjunction with crude oil, in isolated gas fields as well as in coal beds. The different gas types can be seen in figure 2.1.

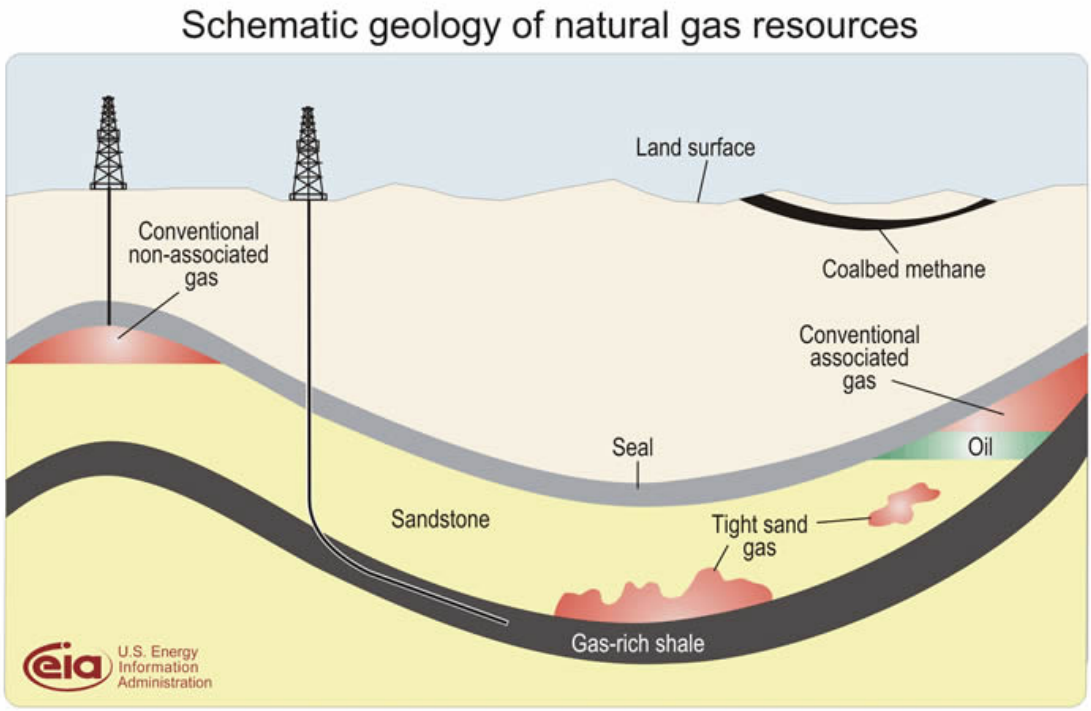

Figure 2.1: Gas resources. Source: U.S. Energy Information Administration.

Currently there are 185.7 trillion cubic meters of proven reserves, but the total recoverable amount of natural gas is estimated to be around 850 trillion cubic meters [30]. Largest proved reserves are in Iran, Russian Federation and Qatar, together

covering almost half of the know reserves. The largest producer, however, is the USA due to the recent growth in shale gas recovery [6].

Biogas is a renewable alternative for natural gas. It is usually produced by decomposition of waste materials such as manure. Capturing the gases released from the decomposition and using them as an energy source provides renewable energy while preventing methane, a more potent greenhouse gas than CO_2 from escaping to the atmosphere. As an example, biogas could replace 5 % of current U.S. natural gas consumption according to [51].

3. ADSORPTION

Adsorption, the adhering of one substance on the surface of another, has been academically studied since the late 18th century, with the first theoretical models emerging in the early 20th century [14]. Applications for adsorption range from purification or separation of gases and liquids, being used as a catalyst, used as a heat storage, and to heat pumps based on adsorption. Moreover, the application that is the main motivator for this work, as a gas storage method.

3.1 Theoretical background

3.1.1 Adsorption as a phenomenom

Adsorption is defined by IUPAC as 'increase in the concentration of a substance at the interface of a condensed and a liquid or gaseous layer owing to the operation of surface forces' [46]. The fundamental idea is that moleules adhere to a surface, where they take less space than they would take in gas phase. It is a phenomenom that may happen between liquid-liquid [58], gas-liquid [44], liquid-solid [27], and gas-solid interfaces [60]. The most important terms used to describe the adsorption phenomenom are defined in table 3.1.

Adsorption should not be mixed with absorption: Adsorption is a surface phenomenom, while absorption takes place in the bulk volume of the absorbent. Absorption may take place between a gas or a fluid that is absorbed to a gas, fluid or

Table 3.1: Definition of terms related to adsorption.

Term	Definition
Adsorption	Adhesion of a material on the surface of another material.
Desorption	Opposite of adsorption, the decrease in the adsorbed phase.
Sorption	Adsorption, absorption or ion exchange process.
Adsorbent	The bulk material on which the adsorption takes place.
Adsorbate	The adsorbed material.
Adsorptive	A material that is capable of being adsorbed.

solid. Sorption can be used to mean both adsorption and absorption. The difference between adsorption and absorption can be seen in figure 3.1.

In this work sorption is used interchangeably with adsorption.

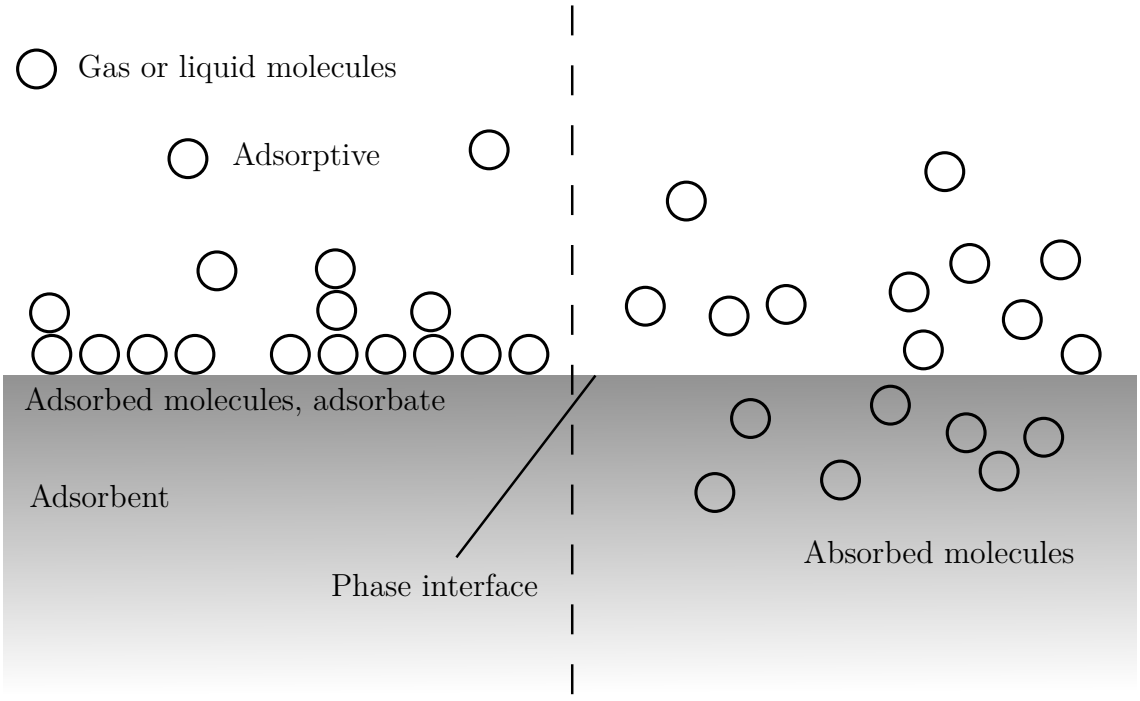

Figure 3.1: Adsorption and absorption. Left: Molecules adsorbed on a phase interface. Right: Molecules absorbed inside another phase. Based on [37].

Two types of adsorption can be observed: chemisorption and physisorption. A comparison of these can be seen in table 3.2. Chemisorption includes a chemical reaction between the susbstance being adsorbed, the adsorbate, and the substance it is adsorbed to, the adsorbent [47]. In physisorption however, the adhesion is caused only by physical forces such as the van der Waals force, as in due to permanent dipoles, a permanent and an induced dipole or between two induced dipoles. Adsorption energy defines how strong the bond is. The reaction is typically exothermic for adsorption and endothermic for the opposite reaction of adsorption, desorption. The energy involved is typically much higher for chemisorption due to the chemical nature of the bond, yet this is not always the case. In some cases the adsorption reaction may even be endothermic, yet these are limited to only chemisorption [71].

This work focuses on using adsorbents as a storage material for gases. Therefore, adsorption is defined in this work as physisorption on a gas-solid interface. The interatomic potential caused by van der Waals forces can be described with the Lennard-Jones potential

$$\phi_{LJ} = 4\epsilon[(\frac{\sigma}{r})^{12} - (\frac{\sigma}{r})^{6}], \tag{3.1}$$

Table 3.2: Physisorption and Chemisorption [60].

Physisorption	Chemisorption
Low heat of adsorption. Typically < 50 kJ/mol	High heat of adsorption. Typically > 500 kJ/mol
Non specific.	Highly specific.
Monolayer or multilayer.	Monolayer only.
No dissociation of adsorbed species.	May involve dissociation.
Only significant at relatively low temperatures.	Possible over a wide range of temperatures.
Rapid, non-activated, reversible.	Activated, may be slow and irreversible.
No electron transfer although polarization of sorbate may occur.	Electron transfer leading to bond formation between sorbate and surface.

where ϕ is the potential, ϵ is the depth of the potential well, σ is the distance where the intermolecular potential is zero and r is the distance between the particles [60]. The 12th power term represents the repulsive force and the 6th power term represents the attractive force. The ϵ and σ are molecular specific constants. For larger molecules a form of

$$\phi = \frac{A}{r^{12}} - \frac{B}{r^6} \tag{3.2}$$

can be used, with the semi-empirical constants A and B.

The effect of electrostatic energies are significant in ionic adsorbents. Energy from polarization can be expressed as

$$\phi_p = -\frac{1}{2}\alpha E^2, \tag{3.3}$$

the field-dipole as

$$\phi_\mu = -\mu E, \tag{3.4}$$

and the field gradient-quadrupole as

$$\phi_Q = \frac{1}{2}Q\frac{\partial E}{\partial r} \tag{3.5}$$

where E is the electric field, α the polarizability, and μ the dipole. The quadrupole moment Q is defined as

$$Q = \frac{1}{2} \int q(\rho, \theta)(3cos^2\theta - 1)\rho^2 dV, \tag{3.6}$$

where $q(\rho, \theta)$ is the local charge density. The complete potential for a molecule is therefore

$$\phi_{tot} = \phi_{LJ} + \phi_p + \phi_\mu + \phi_Q + \phi_s, \tag{3.7}$$

where ϕ_s represents the interactions between the sorbates. For low coverage adsorption, this is approximately the heat of adsorption. For low coverages adsorption follows the Henry's law. In higher pressures a different approach is required. [60]

As pressure increases and adsorption progresses, at some point the pores become filled with fluid at a a pressure lower than the saturation vapor pressure of the fluid. This phenomenom is called capillary condensation, and it can be clearly seen in the adsorption behavior of CO_2 on some porous materials [75]. This effect also may cause hysteresis loops, where the adsorption and desorption behaviors are not similar. Methane is not affected by capillary condensation into macropores in ambient temperatures and pressures due to its low critical point [28].

The adsorbed amount can be defined in three ways: total, absolute and excess adsorption. The difference between these types is illustrated in figures 3.2 and 3.3.

Figure 3.2 describes the situation inside a pore of a solid material. The black line on the bottom of the figure describes the surface of the solid and the circles above is area gas particles. On the left part of the figure there are three types of gas particles: 'a', 'b', and 'c'. The black a particles are adsorbed on the solid surface. Free gas particles in the bulk phase are described with 'c', while 'b' describes the gas particles that are in the volume where adsorption takes place, yet that are not adsorbed. On the right side the density distribution of the gas can be seen: The bulk gas 'c' has a certain density that is the same as with the the 'b' particles. Adsorption causes an increase in the gas density near the surface of the solid. If no wall effects ie. adsorption took place, the a part on neither side would exist and the density would be independent of the distance from the solid surface.

The part 'a' is therefore called the excess adsorption. Absolute adsorption includes both the 'a' and 'b', whereas the total adsorption covers all 'a', 'b' and 'c'. The excess adsorption is what can be measured with the setup used in this work. It can be considered as a kind of efficiency of adsorption: how much gas uptake does the adsorption provide compared to a situation with no wall effects. Absolute adsorption is what can be calculated when simulating adsorptive behavior, yet the term has little other use. Total adsorption includes all the gas inside the pores, both the bulk

gas and the adsorbed part. Therefore total adsorption is the most useful term when describing gas storage: It directly shows the gas uptake of a porous material.

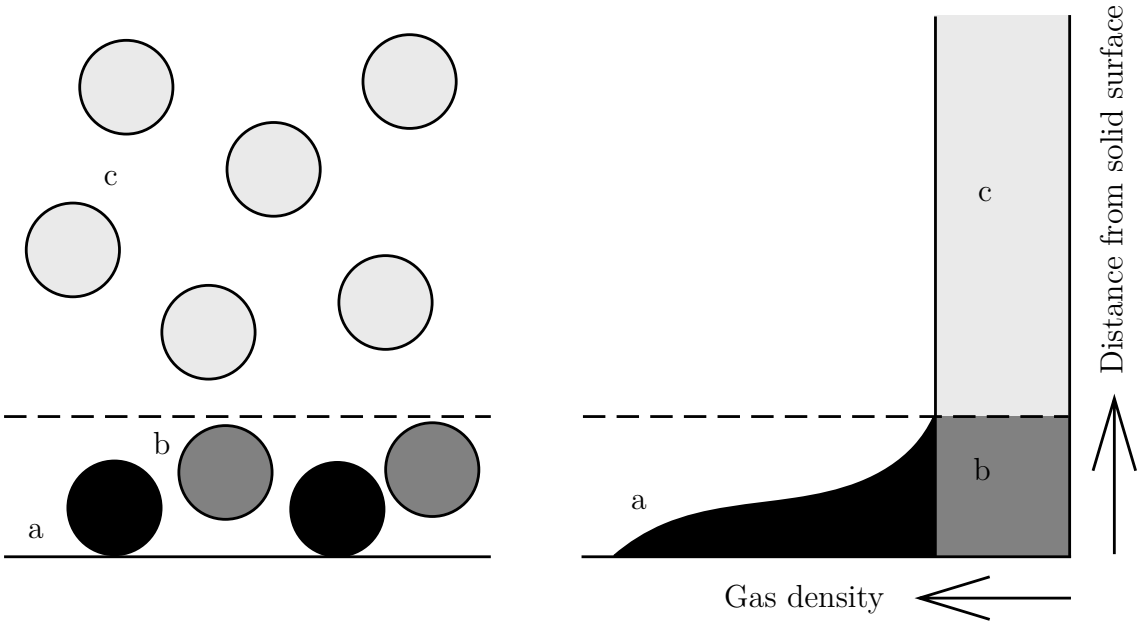

Figure 3.2: Adsorption on a pore surface. a: adsorbed gas particles. b: bulk gas particles near the surface. c: bulk gas. Left: description of the particles. Right: gas density as a function of distance from the wall. Adapted from [45].

Figure 3.3 shows the adsorption isotherms for the different adsorption types. All three curves have the same rapid increase in the beginning. The excess curve reaches a maximum value, after which it starts to decline. This decline comes from the density of the bulk gas nearing that of the adsorbed layer. This effect can be seen in the equation

$$m_{ex} = m_a - \rho_m V_a, \tag{3.8}$$

where m_a is the absolute adsorption mass, ρ_m is the density of the bulk fluid phase and V_a is the volume is the adsorbent [45]. As the bulk density increases, the absolute adsorption stays relatively the constant but the excess adsorption decreases. In figure 3.2 this can be seen as the ratio between a and b becoming smaller.

The absolute adsorption curve in figure 3.3 rises rapidly and the levels to a certain value. The total adsorption curve increases indefinitely as the pressure increases, in the same way as the uptake would increase in a case with only gas compression and no wall effects.

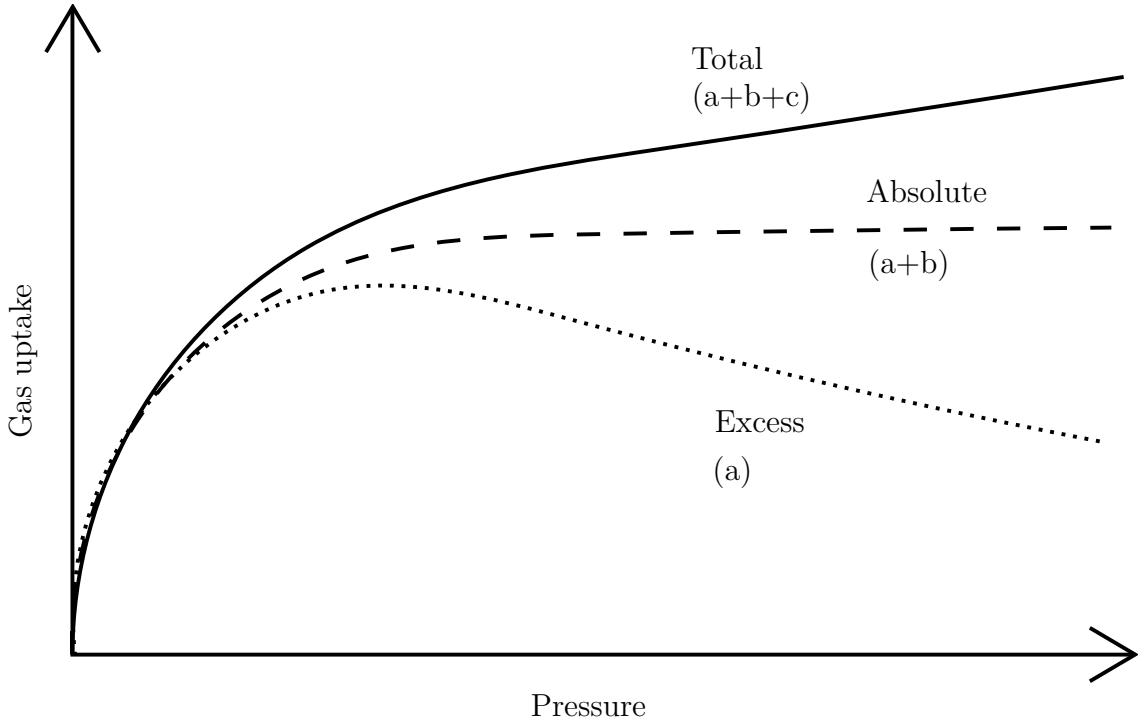

Figure 3.3: Total, absolute and excess adsorption. Adapted from [66].

3.1.2 Adsorption isotherms

Adsorption is a highly temperature dependent phenomenom. Typically adsorption is an exothermic process, and the adsorbed amount is decreased with increasing temperature [3]. Therefore adsorption is usually characterized with adsorption isotherms that describe the equilibrium state at the phase interface at different pressures and at a constant temperature. The adsorbed amount is typically measured in volumes per volume of adsorbent or in grams adsorbed per gram of adsorbent.

According to IUPAC classification there are 6 basic types of adsorption isotherms [62]. These isotherms are shown in figure 3.4.

Type I depicts adsorption monolayer formation and is common in gas adsorption on microporous solids. Type II does not exhibit the same kind of saturation that type I does, and it depicts multilayer adsorption on a non-porous solid, yet in some cases microporous solids may exhibit these kinds of isotherms. The point B refers to the formation of the adsorption monolayer. Type III isotherms are typical for non-porous or macroporous solids with weak gas-solid interactions. Isotherm type IV is similar to type II but includes capillary condensation and a hysteresis loop, which makes the desorption curve different from the adsorption curve. Type V is similar to type III but includes the hysteresis. Type VI exhibits stepwise behavior and is usually a combination of the other types of isotherms.

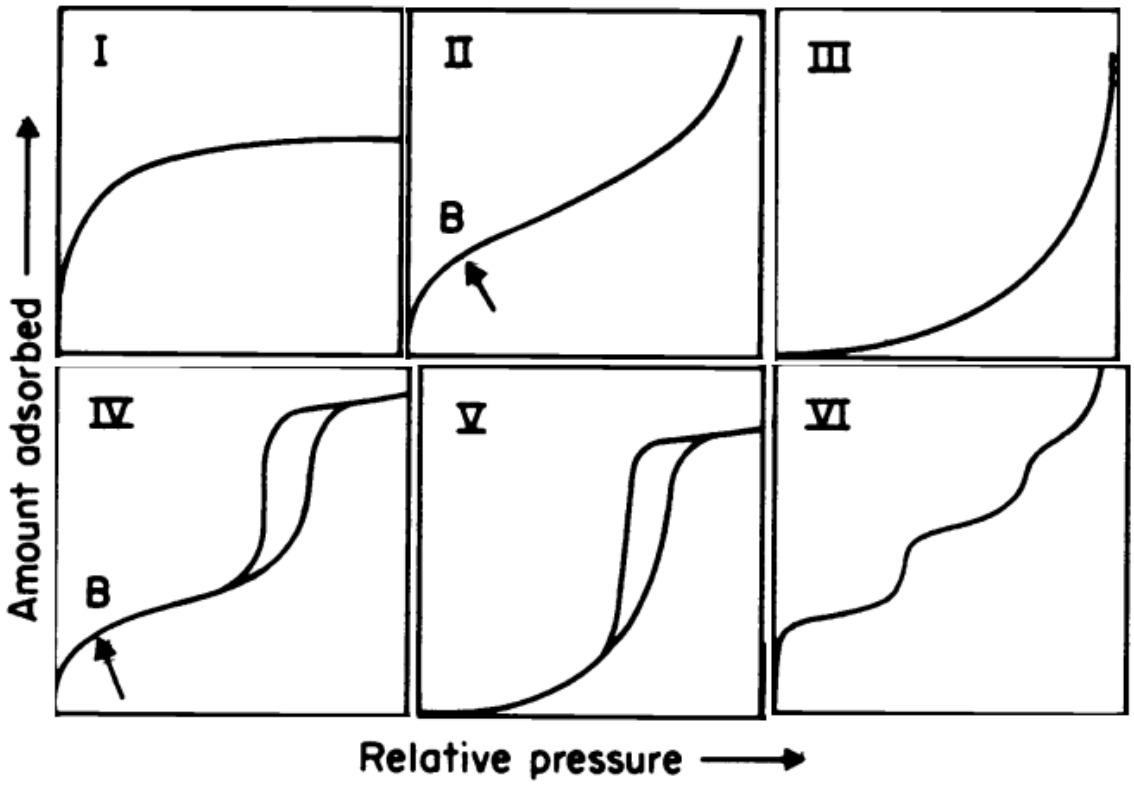

Figure 3.4: IUPAC classified adsorption isotherms [62].

The Freundlich adsorption isotherm is the first developed equation describing adsorption. It is a simple, empirical equation describing the adsorbed amount adsorbed per amount of adsorbent, X/m, in different pressures. It is defined as

$$\frac{X}{m} = kp^{\frac{1}{n}}, \tag{3.9}$$

where X is the adsorbed amount, m is the amount of the adsorbent, p is the pressure and k and n are substance and temperature specific rate constants [37].

The Langmuir adsorption isotherm is based on a number of assumptions. The adsorption may happen only at specific identical points on the surface and the previously sorbed particles do not affect the adsorption of the other particles. The model does not take into account surface roughness or multilayer formation, but it is still one of the most used adsorption isotherms. The Langmuir isotherm has the form

$$\theta = \frac{(\frac{k_a}{k_d})p}{(\frac{k_a}{k_d})p + 1}, \tag{3.10}$$

where θ is the surface coverage of the adsorbate, p is the pressure and k_a and k_d are rate constants for adsorption and desorption reactions [74].

Brunauer, Emmett and Teller (BET) extended the Langmuir theory to multilayer adsorption by applying the Langmuir equation for each layer [7]. The isotherm has the form

$$\frac{X}{X_m} = \frac{C(p/p_0)}{(1-p/p_0)(1+(C-1)p/p_0)}, \tag{3.11}$$

where X is the adsorbed mass, X_m the mass of the adsorption monolayer, C refers to relative lifetime of molecules in the condensed state and p and p_0 are the pressure and saturation pressure of the adsorbate. The BET theory include the assumptions that the gas may form an infinite amount of adsorpbed layers and that the molecules between the layers do not interact. One could think that the term $\frac{X}{X_m}$ equalling one would mean that a full coverage has been achieved. However, multilayer adsorption may start before a full monolayer has been achieved. [22]

The BET isotherm is of much interest, as it is commonly used in determining the specific surface area, or otherwise known as the BET surface area S_{BET} of a substance which can be calculated from

$$S_{BET} = \frac{X_m}{M} N A_m, \tag{3.12}$$

where M is the molar weight of the adsorbate, N is the avogadro number and A_m is the area occupied by one molecule in the monolayer. [7]

BET surface area is not the same as the real, physical surface area of a substance, but only a characteristic number that reflects the surface area. The values may vary greatly for different substances, surface textures and pore sizes, but the BET area is still an invaluable tool in surface area determination. The experimental determination of the BET area is discussed later. The Langmuir theory can be used for surface area determinations as well, but it is more suitable for chemisorption. It also differs from the BET area calculated for the same substance. [40]

A large number of other isotherms exist, based on different theoretical principles and that are valid in different pressure ranges. These isotherms are reviewed in [24].

3.2 Adsorbent materials

As adsorption is a surface phenomenom, the single most important factor for an adsorbent is its specific surface area (SSA). It is the total surface area of a solid per unit of mass, usually denoted as m^2/g. The SSA can be as high as 7000 m^2/g for Metal-Organic Frameworks (MOF) [23], activated carbons (AC) are typically in the range of 500-3000 m^2/g.

Specific surface area is affected by grain size, shape, surface roughness and porosity. Out of these, for gas storage applications the most important one is porosity.

Figure 3.5 shows different kinds of pores inside a solid. Closed pores are completely surrounded by the bulk material, having no connection outside or to other pores. Open pores are accessible from outside. Blind pores are 'dead ends', through pores are pipe-like and are open on more than one end. The pores can also be interconnected. The pores may have a round cross section, they may be ink-bottle shaped with a wide body and a thin neck or they may be slit-shaped. These pore shapes are important in many modelling assumptions.

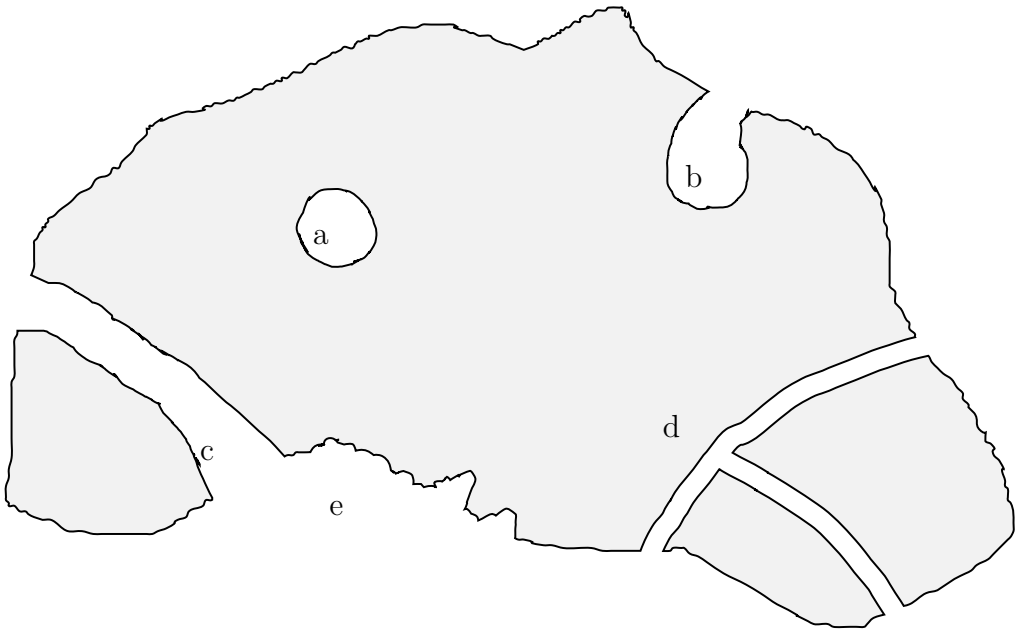

Figure 3.5: Porosity. a: closed pore. b: open, blind pore. c: through pore. d: through, interconnected pores. e: surface roughness.

IUPAC classifies pore sizes to three groups that can be seen in table 3.3. Different pore sizes are usually present in a porous solid. It has been suggested that the optimal pore size for methane storage applications would be around 0.8 nm, larger than the size of two methane molecules [42]. Cracknell et al. [13], however, suggest that a pore size of 1.14 nm would provide a better delivery at 34 bar.

Chang et al. classify the most important adsorbents for gas storage applications into three groups: Carbonaceous materials, organic frameworks and zeolites.

Table 3.3: Classification of pores by their diameter [59].

Classification	Pore diameter		
Micropores	0 nm	< d <	2 nm
Mesopores	2 nm	< d <	50 nm
Macropores	50 nm	< d	

Table 3.4: Definitions of different types of densities.

Density	Description
True (skeletal)	Density of the solid material, including closed pores.
Apparent	Density of the material, including open and closed pores.
Bulk	All pores and interparticle voids are included. Packing density.

3.2.1 Carbonaceous materials

Activated carbons (AC) are popular adsorbents due to their good availability and relatively good adsorption capacities [14]. The precursor materials for activated carbons are abundant, as AC can be produced from most carbonaceous materials, commonly from waste materials such as fruit stones or coconut husks [36]. The process of producing activated carbon requires selective gasification of the precursor material. Carbonization is done under an inert atmosphere and in the presence of an activating agent such as phosphoric acid or steam. The inert atmosphere is used to prevent most of the carbon from reacting to carbon dioxide, which would otherwise lower the yield. Normal carbons that are produced only with heat treatment have low surface areas and the activating agents are used to increase this area. Depending on the carbonization temperature, heating rate, and the activating agent, different porosity distributions can be achieved from a single type of precursor material. These properties may be optimized for what ever the product is meant for, such as water or gas purification or gas storage.

The activated carbons produced for this work were activated with phosphoric acid according to [32]. According to the article, the phosphoric acid promotes bond cleavage reactions and the formation of crosslinks along with connecting biopolymer fragments, expanding the material and providing a better pore structure. Various other activating methods exist in addition the one used [4].

Activated carbon may be in the form of powders, granules or monoliths. Monoliths are typically extruded pellets made from powdered activated carbon and some binder agent. Some methods exist to prepare binderless monoliths [57]. Monoliths have the advantage of having a much better packing density due to decreased interparticle voids compared to powdered or granular form [41].

A relatively recent type of carboncaeous adsorbents are zeolite-like carbon materials.

They are prepared by depositing carbon to a hard zeolite template using Chemical Vapor Deposition. The carbon precursor is typically acetylene due to its high reactivity. This method allows the production of adsorbents with the positive properties of both carbons and zeolites.[2]

Other carbon materials that have been researched as adsorbents include single- and multi-walled carbon nanotubes. These have proven to be especially interesting in hydrogen storage applications [76].

Catalytic decomposition of methane is a process where methane is decomposed into gaseous hydrogen and solid carbon in high temperature and in the presence of a catalyst. As mentioned by Fager-Pintilä (2012), there would be a huge surplus of carbon should this technology be technologically viable. It would be of interest to find out whether the carbon produced by TDM could be used as an adsorbent for storing methane or carbon dioxide, either directly or after some form of treament. Other relatively cheap precursor materials might be available in the form of biochar from the production of pyrolysis oil.

3.2.2 Organic frameworks

Metal-organic frameworks (MOF) have been widely studied as an adsorbent during the recent 20 years. They are constructed from metal nodes connected by organic bridges, and may be easily tailored for specific applications. It is this tailoring that gives MOFs their biggest advantage: the pore sizes can be tuned precisely and the functional groups can be chosen according to the chosen adsorbate. The tailoring is much more easily done for MOFs than for ACs or zeolites [43]. Farha et al. have theorized a maximum hypothetical surface area of 14 600 m^2/g for MOFs in addition to the highest synthesized 7000 m^2/g material [23].

3.2.3 Zeolites

Zeolites are aluminosilicate materials used commonly as adsorbents, molecular sieves and catalysts. They have been broadly studied for adsorption storage and separation, especially for CO_2 storage. Zeolites suffer from structural limitations, have relatively low specific surface areas (up to 1000 m^2/g) and have problems with losing their gas adsorption properties due to preferential adsorption of moisture [48]. These properties generally make zeolites unattractive for storage purposes.

3.3 Applications

Adsorption is used in multiple different application ranging from storage, being used as a catalyst and to purification and separation of gases and liquids.

3.3.1 Adsorption storage

One of the major motivations behind this study comes from the proposition that ANG could be used as a large scale passive storage method as a part of the gas transport network [35; 61]. ANG does not require the constant cooling that LNG needs to stay liquid and can store higher amounts of gas in lower pressures than CNG. Passive CNG storage attached to the network could store very little methane compared to the material costs and compressing it to a higher pressure for storage would require energy, multi-stage compressors and sturdier containers which would raise the investment costs.

When filling an adsorption storage with natural gas, the gas must first flow through a 'guard bed' as proposed by [12]. Higher hydrocarbons along with other impurities have a tendency to adsorb more easily and are difficult to desorb. This would cause storage deterioration over time by reducing the methane storage potential. Therefore the gas is first passed through a regeneratable or switchable adsorbent bed. When emptying the storage, the guard bed could be heated to desorb the sorbed components back into the stream.

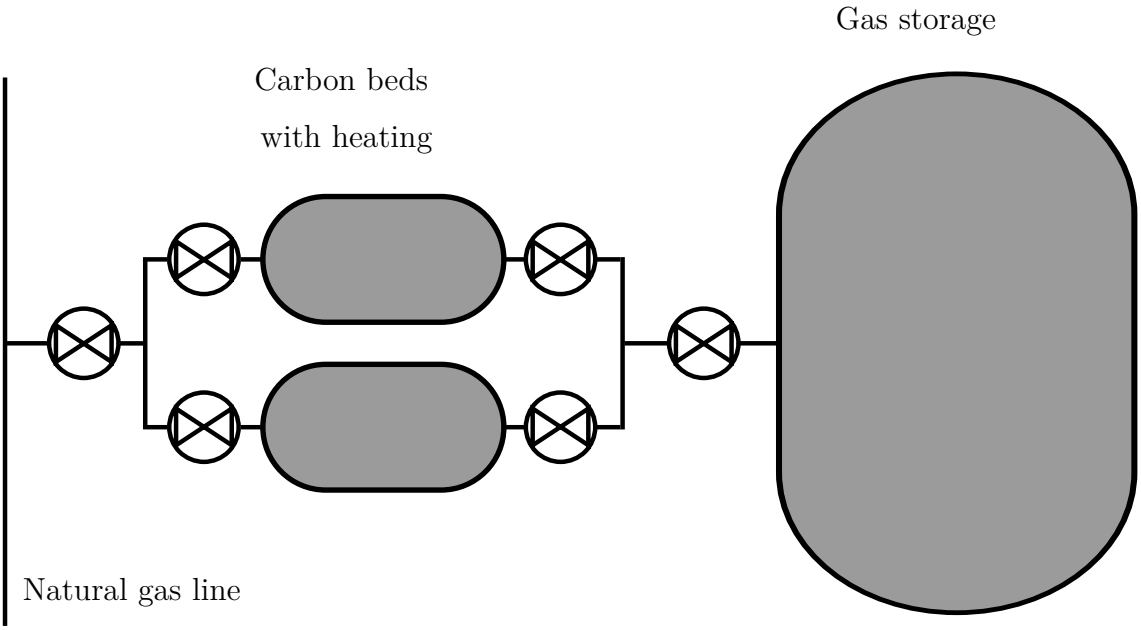

Figure 3.6: Natural gas passive storage connected to transport pipeline. Adapted from [12].

Major challenges in large scale adsorption storage include dealing with heat changes in the bed during adsorption and desorption, degradation of the adsorbent due to heavier hydrocarbons and the presence of moisture, pressure loss in the bed, and optimal pore structure that allows both high adsorption capacity and high gas

transport capabilities within the bed. Purely microporous adsorbents can store more gas, but without macropores the loading and emptying of the storage is far too slow for practical purposes. [35; 68]

ANG has been proposed for vehicular use to replace the currently used CNG technology [12]. With higher storage capacity in lower pressure compared to CNG, it may allow savings in both the fuel container construction and in fueling station compressors. The ability to build gas containers to a shape different from cylinders allows more efficient use of space in the vehicle.

Stationary ANG differs greatly from vehicular applications. For vehicles, both volumetric and gravimetric energy densities are of great importance. For large scale storage however, greater focus is on the price and its mechanical properties. [61]

Hydrogen storage in adsorbents has been studied widely and is of great interest. Hydrogen storage can typically be done by liquefaction, chemical storage or using adsorbents. Temperature and pressure requirements for the liquefaction make it unfeasible in most cases. Chemical storage poses problems with reversibility, kinetics and heat management. The enthalpy associated with adsorption is much lower than the enthalpy change in chemical reactions, which helps with the reverisibility and heat management problems. [49]

According to Morris et al. the adsorption storage of other gaseous hydrocarbons such as acetylene has been studied much less than the storage of the other gases mentioned in this work [49]. They do, however, show potential as well compared to conventional storage methods. The storage of other gases such as nitric oxide are discussed in the same article.

Temporary CO_2 storage has been suggested to be used with load following power plants to help with carbon capture and storage (CCS) methods. As the load following power plants are not run constantly, CO_2 is not produced at a constant rate. The CO_2 needs to be compressed prior to transporting. The temporary storage could reduce the instantaneous capacity needed for the compression, as the stored gas could be released at a constant rate or over a longer time.

An interesting application of adsorption storage is to not store gas on an adsorbent, but to use the adsorbent itself as an energy storage. When energy is needed, water vapor is allowed to adsorb onto an adsorbent like zeolite which releases energy. To 'store' energy, the adsorbent is heated which releases the adsorbate, preparing it for further use [33].

3.3.2 Gas separation and purification

Pressure swing adsorption (PSA) is a relatively simple, yet broadly used method for gas separation. In high pressures certain components are adsorbed on the adsorbent, enriching the other components in the gas flow. To regenerate the adsorbent, the pressure is lowered so that the previously adsorbed components desorb, enriching the gas flow with that component. PSA is typically utilized in a multiple column system, where one column is used while the others are being regenerated. [63]

Instead of between ambient and a higher pressure, PSA can done between ambient pressure and vacuum which is called vacuum swing adsorption (VSA) or between vacuum and a positive pressure which is called vacuum pressure swing adsorption. All of these are referred to simply as PSA in this text.

Pressure swing adsorption is commonly used in purification of hydrogen and in nitrogen and oxygen generation. It can be used in purification of biogas to remove hydrogen sulfide and to adjust the CO_2/CH_4 -ratio [1]. PSA has also been studied in concentrating and recovering CO_2 from flue gases with multiple different adsorbates [11; 39]. Air separation is typically done with cryogenic distillation, which is only viable with high volume flows. For smaller volume flows, PSA is more viable as it can be scaled down to even portable separators and can be used in applications with less strict gas purity requirements.

Adsorption is used in most respirators and gas masks to remove small particles and harmful gases from the inhaled air. Common usage for AC filters can be found as personal protective equipment in military applications, industrial and personal use.

3.4 Characterization

Characterizing porous substances is of great importance, as it allows one to determine the properties that affect adsorption. Specific surface area alone does not reveal the adsorption capacity, but a combination of a high surface area along with optimized pore structure and a suitable material density can provide high adsorptive properties.

3.4.1 Mercury porosimetry

Mercury is a much-used fluid for porosimetry due to its non-wetting properties. Mercury porosimetry can be used to determine the pore size distribution, total pore volume, specific surface area, and the apparent density of a material. It can be used for pore sizes between 500 μm and 3.5 nm, yet closed pores are naturally beyond its

reach, as are some ink-bottle pores with neck smaller than the allowed mimimum pore size.

The sample is immersed in mercury and is subjected to various levels of pressures. At every pressure the amount of mercury required to fill the pores is measured. The smaller the pores, the higher is the pressure needed to overcome the surface tension of mercury.

Washburn equation, which is a modified form of the Young-Laplace equation, describes the pressure difference Δp across the mercury interface. This equation is expressed as

$$\Delta p = \gamma(\frac{1}{r_1} + \frac{1}{r_2}) = \frac{2\gamma \cos\theta}{r_{pore}}, \tag{3.13}$$

where r_1 and r_2 describe the curvature of the mercury interface, r_{pore} is the pore radius corresponding to the current pressure, γ is the surface tension of mercury, and θ is the contact angle between mercury and the sample material. A major assumption made in this model is that the pores are cylinder shaped. Usually this is a good approximation, but in some cases it may distort the results. [26]

3.4.2 Gas pycnometry

Typically performed with helium, gas pycnometry is a method used to measure the volume of a substance. Due to its size, helium can enter pores down to 0.1 nm range, giving it a much better range and accuracy than that of mercury porosimetry. True density of a substance can be determined from the measured volume when the mass of the sample is known. Gas pycnometer is limited to only volume measurements: pore size distribution along with surface area are beyond its reach because filling of smaller pores requires no increase in pressure for helium as it does with mercury. A typical setup can be seen in figure 3.7.

The basic principle is to fill a sample-loaded vessel with helium to a certain pressure. Then a valve to the reference volume chamber is opened and the pressure is again measured. The volume V_s of the sample can be calculated from the equation

$$V_s = V_c + \frac{V_r}{1 - \frac{p_1}{p_2}}, \tag{3.14}$$

where V_c is the volume of the sample vessel, V_r is the reference volume and p_1 and p_2 are the pressures prior and after the valve opening, respectively. [8]

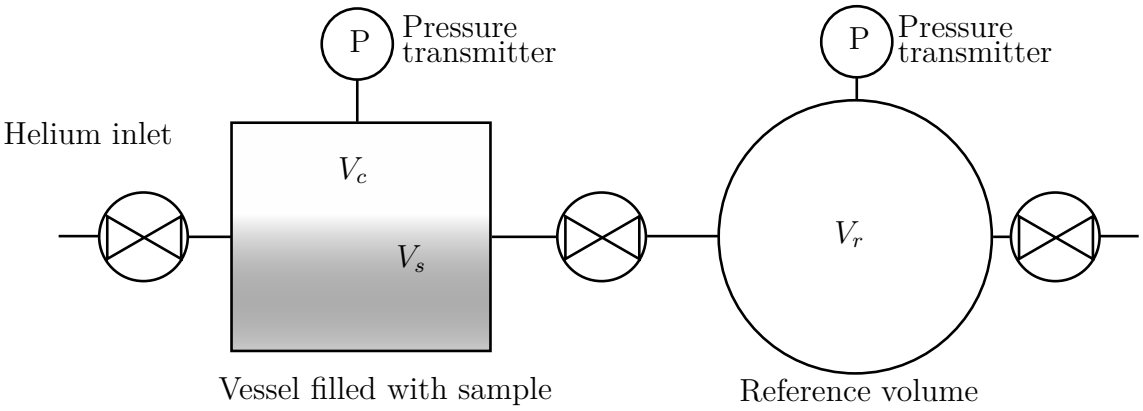

Figure 3.7: Gas pycnometer. Adapted from [8].

3.4.3 Adsorption measurements

Adsorption measurements are typically done with either the volumetric, gravimetric or the continuous flow method. Usually the measurements are done with nitrogen at the temperature of 77 K. Reaching the adsorption equilibrium may take time, and determining the state can be difficult. Therefore a 'technical equilibrium' is defined, which is close enough to the true equilibrium for the results to be usable in practical applications. The time required to reach the equilibrium greatly depends on the substances examined. [37]

A setup for the volumetric adsorption method can be seen in figure 3.8. The measurement procedure involves first determining the total void space inside the sample vessel. This can be calculated from the volume of the vessel and the true density of

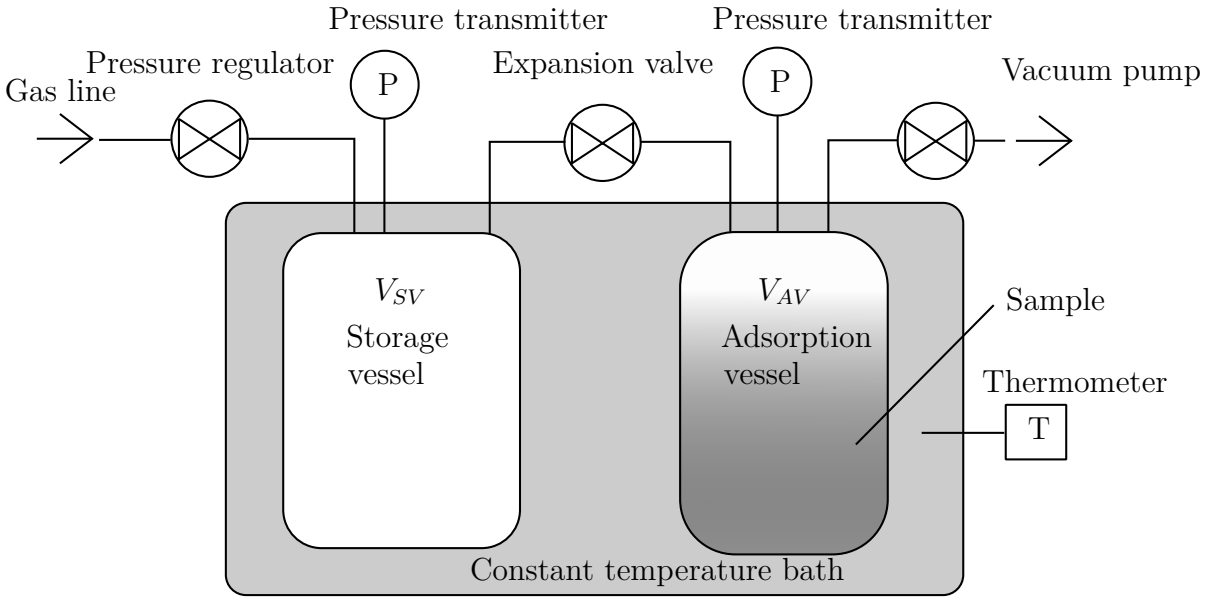

Figure 3.8: Adsorption measurement with the volumetric method. Adapted from [37].

the sample or directly in a manner similar to helium pycnometry. Then the storage vessel is filled to a certain pressure with the adsorptive gas. The pressure is measured and the expansion valve is opened so that the gas enters the sample-filled vessel. The pressure is measured again. If some of the gas is adsorbed on the sample, the pressure will be lower than with a non-adsorptive gas.

The true density is typically measure with helium, as it can be considered non-adsorbing in room temperatures [50]. Downsides of the volumetric method include the requirement for the density measurement and the need to calibrate for adsorption on container walls.

Gravimetric adsorption measurements are typically done by directly measuring the adsorbed mass by weighing the sample. A typical setup can be seen in figure 3.9. Sophisticated magnetic suspension balances are used, with an accuracy up to 10^{-8} g. Thanks to the magnetic coupling, the sample can be directly weighed even in high pressures, high temperatures and corrosive atmospheres. The temperature and pressure are constantly measured, and they are needed to correct for buoyancy.

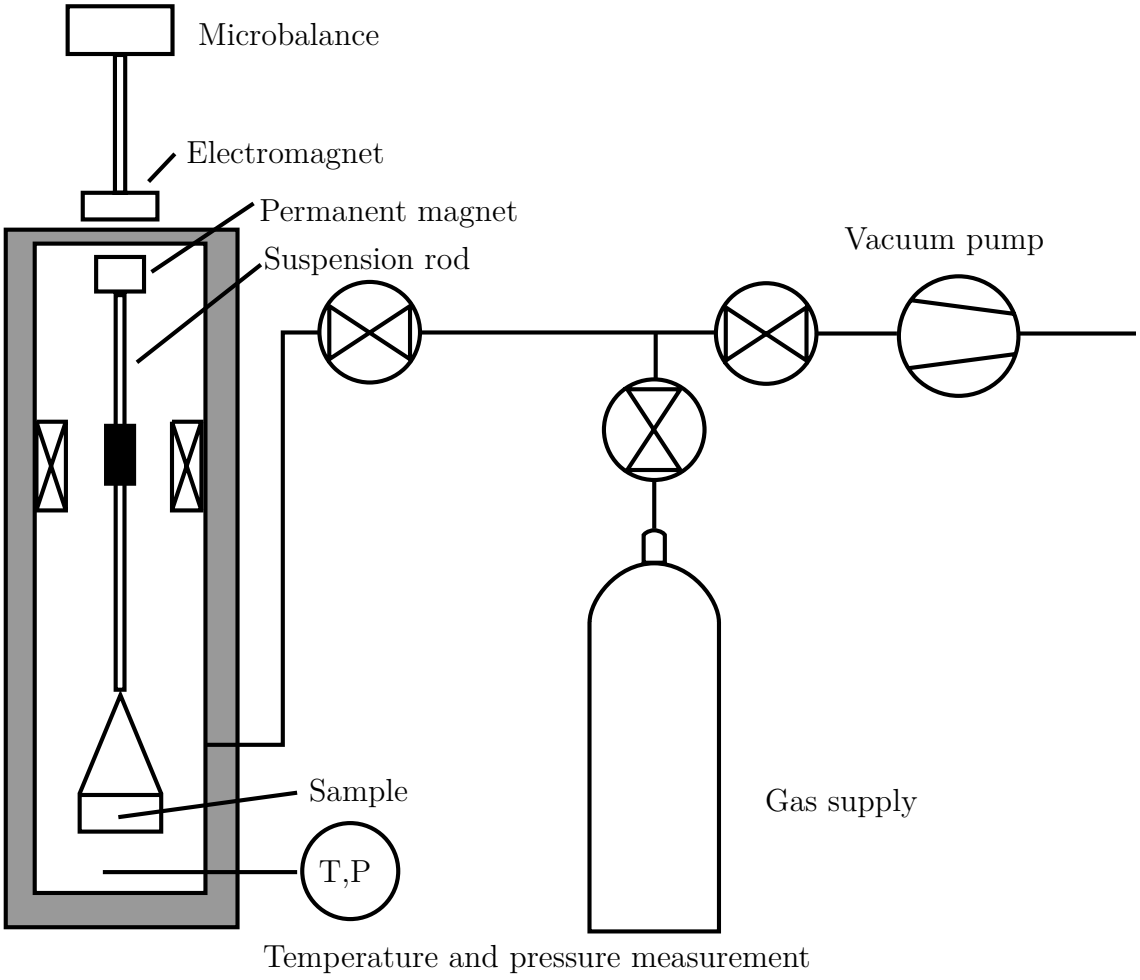

Figure 3.9: Adsorption measurement with the gravimetric method. Adapted from [37].

Volumetric method is much simpler and cheaper than the gravimetric. Microbalances are expensive and the operation of the gravimetric setup requires constant supervision as it cannot be easily automated. Compared to the volumetric method, gravimetric approach provides a better accuracy and much smaller required sample size.

Oscillometry is a more recent method used in adsorption measurements. A torsional pendulum has the examined adsorbent attached to it and the pendulum is rotated in a selected gas atmosphere. As the gas adsorbs on the adsorbent, the moment of inertia of the pendulum changes. This affects its oscillation and the change can be measured. [37]

3.4.4 Impedance spectroscopy

Temporary polarization takes place in a a dielectric material if it is exposed to an electric field. If the field is alternated, the change rate in the polarization can be measured with impedance or capacitance measurements. Using alternating, variable electric fields, characteristic curves specific to the adsorbate/adsorbent system are aquired, which allow the determination of the current state of sorption. This method can be combined with volumetric, gravimetric or oscillometric methods to determince excess amount adsorbed. [37; 65]

3.4.5 Small-angle scattering

Small-angle X-ray scattering (SAXS) and small-angle neutron scattering (SANS) are methods used to study the porosity of materials. These methods are based on targeting either X-rays or neutrons on the examined sample. Most of the rays or neutrons go straigt, but some of them scatter. By measuring the intensity of the scatter in different angles the size distribution of the pores may be measured. These methods can give information on pores with diameter as low as 1 nm. [56]

3.4.6 Real gas correction

The void volume in the measurements performed in this work is calculated from the helium measurements. This volume is used to calculate how much methane would fit in the void space if no wall interactions took place. This reference methane amount, m, is calculated from the real gas equation

$$m = \frac{pVM}{R_u TZ}, \tag{3.15}$$

where p is the pressure, V is the void volume of the container, M is the molar mass, Ru is the universal gas constant, T is the temperature and Z is the real gas factor used to correct for non-ideal gas behavior. The mass is calculated as a reference value for each measured point, by using the measured pressure and temperature and comparing the calculated mass to the measured one.

The Peng-Robinson equation of state is used to calculate the Z-factor to correct for the real gas behavior of methane in higher pressures, as well as a correction for the helium void space measurement [55]. The Peng-Robinson equation of state is expressed in the form

$$p = \frac{R_u T}{v - b} - \frac{a\alpha}{v(v + b) + b(v - b)}, \tag{3.16}$$

where v is the molar volume, the coefficient a is given by the equation

$$a = \frac{0.457235 R_u^2 T_c^2}{p_c}, \tag{3.17}$$

and b by the equation

$$b = \frac{0.077796 R_u T_c}{p_c}. \tag{3.18}$$

T_c is the critical temperature of the gas. The dimensionless constant α is defined as

$$\alpha = (1 + \kappa(1 - T_r^{0.5}))^2, \tag{3.19}$$

where the substance characteristic constant κ is given by

$$\kappa = 0.37464 + 1.54226\omega - 0.26992\omega^2 \tag{3.20}$$

where ω is the acentric factor, describing the non-sphericity of molecules. Reduced temperature T_r is defined as

$$T_r = \frac{T}{T_c}. \tag{3.21}$$

The equation 3.16 can be written in a quadratic form as

$$Z^3 - (1 - B)Z^2 + (A - 2B - 3B^2)Z - (AB - B^2 - B^3) = 0, \tag{3.22}$$

where the coefficients A and B are given by

$$A = \frac{a\alpha p}{R_u^2 T^2} \tag{3.23}$$

and

$$B = \frac{bp}{R_u T}. \tag{3.24}$$

4. EXPERIMENTAL

4.1 Setup

The measurement setup used in this work is based on the gravimetric method, but differs in the way the sample is weighed. Typically a magnetic suspension scale is used to measure the sample directly inside the pressurized vessle. Here, a regular scale is used to weigh the whole pressure vessel. The experiments were made with methane instead of real natural gas. The setup was built at the Tampere University of Technology during the autumn of 2014.

4.1.1 Pressure vessel and piping

The pressure vessel used in the study is an old bomb calorimeter as seen in figure 4.1. The vessel was made in 1979 out of BS 1506-845B stainless steel which is closely related to AISI 316 grade steel. The heating wires and the sample cup were removed from the container. Air inlet and outlet holes were drilled bigger and rethreaded. One of the holes was then plugged and the other used as a gas inlet and outlet and for the instrumentation. A cross pipe fitting with threads was attached to the latter hole. On one branch a K-type thermocouple was installed with a compression fitting, so that the head of the thermocouple was approximately halfway down inside the vessel for as close contact with the samples as possible. One branch of the cross fitting was meant for gas inlet and the other as gas outlet.

On the inlet side a ball valve was installed to be able to prevent gas flow in either direction if needed. Upstream from it, away from the cross, a check valve and a double-end shutoff quick-connect were installed. The quick-connect was installed to allow easy separation of the gas line from the vessel. The check valve was installed to make sure the gas would not flow in the wrong direction in case of a mistake in handling of the setup and to prevent backflow whenever the quick-connect was separated. On the other side of the quick-connect a T fitting was installed with a line to gas cylinders on one branch and a ball valve that enables the evacuation of the gas line on the other branch.

Methane with a purity of 99.995% and helium with a purity of 99.996% were used for the experiments. The gases were provided by the Linde Group. Linde Redline

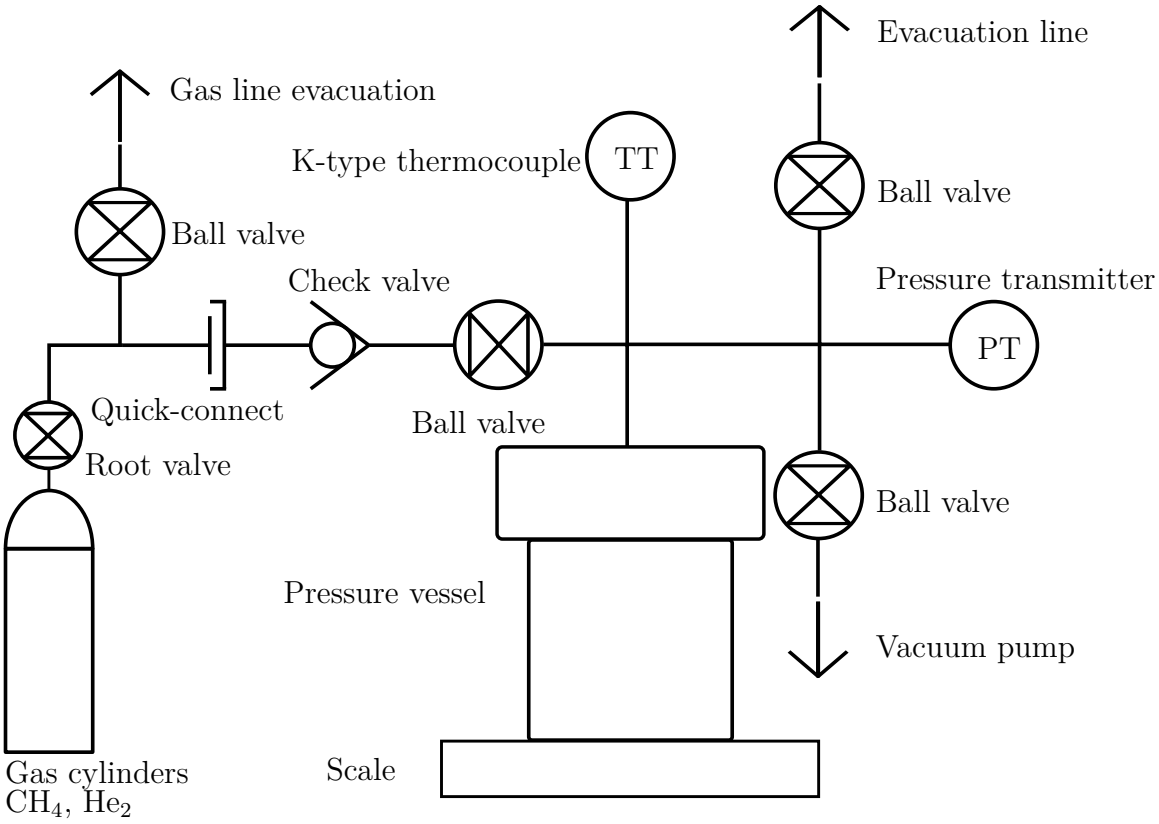

Figure 4.1: Experimental setup.

cylinder regulator C200/1A with a maximum working pressure of 200 bar was used to control the methane pressure.

On the outlet side of the branch are the pressure transmitter and two ball valve protected lines for the vacuum pump and for safely venting the high pressure methane to the atmosphere. The venting line was connected to a fan so that any gases could quickly be vented away from the line. The venting line is disconnected whenever it is not used, and that it remains empty of any flammable gases as air is constantly passed through it. The same line is used for emptying both the vessel and the feed line by moving it wherever it is needed.

All parts except the vessel were made by Swagelok and were connected to each other with 1/4" NPT double nipple connectors. All threads were covered with both thread seal tape and a hardening thread sealant prior to connecting them to achieve gas thightness.

A rubber O-ring was placed between the cap and the vessel to achieve gas tightness. Due to the non-standard size of the O-ring groove of the cap, a perfectly fitting O-ring could not be found. By using silicone grease on the best available O-ring and using enough force when sealing the container, a sufficient gas tightness was achieved. For pressure testing the vessel was pressurized with CO_2 to 50 bar(a),

emptied and then filled with methane to 100 bar(a). All valves were closed and the gas line disconnected. No leakage was detected either by the pressure measurement or the leak detector spraying.

The quick-connect used in the setup can only be connected and disconnected in pressures below 17 bar. Therefore the gas line needs to be emptied after filling the vessel and before disconnecting the quick-connect, using the line evacuation valve.

Robinair 15002 two stage vacuum pump is used to evacuate the system. Despite its age, looking like a relic and constantly spraying out oil, it could evacuate the vessel to a pressure level low enough for this application. That is, a pressure close enough to vacuum.

4.1.2 Instrumentation

An Agilent 34970A data aquisition/data logger switch unit along with a 34901A 20 channel multiplexer was used for data aquisition, connected to a PC through a serial port. A Gems 3100 series pressure transmitter with a pressure range of 0...100 bar and 0.25 % full scale accuracy was used for pressure measurements. A K-type thermocouple was used to measure the temperature. A Radwag PS 6000/C/2/R-WiFi scale with a max capacity of 6000 g, an accuracy and repeatability of ± 0.01g and with internal calibration was used for the weighing. The scale was also connected through serial port.

A measurement software was developed with MATLAB. A graphical user interface (GUI) was developed for further measurements, yet most of the measurements in this work were done with the command line version. The code was constantly improved during the use, and the making the changes was easier to implement on the command line or the editor rather than constantly editing the GUI. Data from the logger could be read by sending in a read request, then requesting the data and finally parsing it. This could be done dozens, if not hundreds of times per second. Measurement data from the scale was fed at a constant rate of 4 measurements per second until the input buffer was filled. This data flow could not be controlled the same way as it works with the data logger, which means that the input buffer needed to be emptied and a moment needed to be waited before aquiring a reading. As only a single reading at each pressure was required, this posed no problem. As the scale had a stabilizing time of some seconds and was therefore not meant for dynamic use, no faster reading rate was required. The requirement for keeping the setup isothermal also allowed some waiting time, while allowing additional time for the system to reach equilibrium.

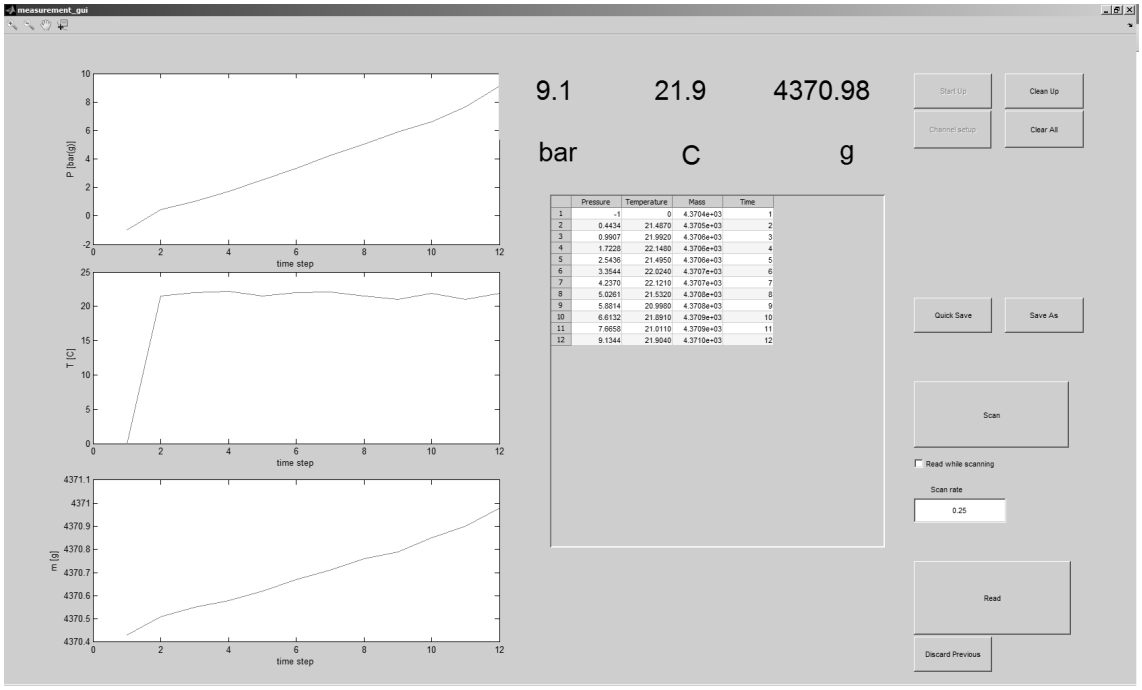

Figure 4.2: Graphical user interface for the measurement software.

4.1.3 Assumptions

Adsorption of helium on activated carbon was assumed negligible. As mentioned in [50] this is not strictly true. Yet, for the purposes of this work this is a safe assumption. And as mentioned in [37], the adsorption of helium on activated carbons may take hours if not days, compared to the minutes it takes to do the calibration.

The inner surface area of the vessel is assumed to be small compared to that of the samples used, and that no adsorption takes place on the walls. The inner surface of the vessel is smoot and its area does not exceed 1 m^2 which is a fraction of the hunders, if not thousands of square meters of the surface area of the adsorbents.

The pressure vessel along with all the connectors are assumed to be rigid. Therefore the volume of the vessel is assumed to be the same in both vacuum and at 80 bar(a). The thermal expansion due to small temperature changes between and during the runs is ignored.

Vacuum pump is assumed to evacuate the vessel to 0 bar(a). The pressure transmitter connected cannot verify this, yet the pump was used in another application and pressures below 0.05 bar(a) were achieved even with some liquid water present in the container.

It is assumed that the samples can be properly degassed. No commercial degassing equipment was available, so heating and multiple evacuations prior to measurements were used. There is no chance to verify the degassing rate with current equipment

and this is one part that should be improved if the setup is used in the future.

4.1.4 Limitations

As mentioned earlier, the whole pressure vessel is weighed instead of just weighing the sample. The vessel along with all the connectors weighs about 4.4 kg. Comparing this to a typical sample size of less than 60 g, the mass of the high pressure methane the vessel will contain of 20 g, and the total amount being adsorbed of around 1 g, it can be seen why systems using magnetic suspension scales are more common than the one built for this work. As the resolution of the scale is 0.01 g, it is multiple orderds of magnitude worse than the 0.01 μg resolution of a magnetic suspension scale.

The uncertainty of the pressure transmitter is low when measuring lower pressures. A full scale accuracy of 0.25 % with 100 bar maximum pressure gives an accuracy of 2.5 % at 10 bar and at 1 bar the uncertainty is 25 %.

Because of the large mass of the container and the relatively good heat transfer properties of steel it is made of, the accurate measurement of the adsorption enthalpy is not possible. Adjusting the temperature is not possible either: heating the gas prior to injecting it into the vessel would do little to heat up the vessel. If the vessel is cooled down to measure adsorption in lower temperatures, condensing moisture will affect the reading, most likely in the same magnitude as the gas addition is.

Currently the setup is suitable only for pure, single gas adsorption. Studying adsorption selectivity or gas separation would require significant changes to the setup. Possibly this could be achieved by capturing the gases when emptying the vessel and analyzing them with a gas chromatograph or FTIR. However, this is no feasible at the moment.

4.1.5 Safety concerns

As very high pressures are used in the setup, some safety concerns had to be taken in account. The pressure vessel, being an old bomb calorimeter, is rated for a pressure of 300 bar. Gas line from cylinders to the quick-connect is provided by Finn-Gamec and is rated up to 400 bar. Pipe fittings provided by Swagelok are rated to over 400 bar.

The quick-connect is rated to 200 bar when connected, but only 17 bar when disconnected. This can be considered one of the most dangerous parts in the system, as the line needs to be remembered to be emptied before attempting to disconnect the quick-connect. The quick-connect needs to be securely connected before trying to

re-pressurize the system as well. These are left to the operator and therefore prone to human error. As a precaution, the line evacuation valve is always left open after the evacuation and until the quick-connect is reconnected to allow a safe exit in the case of an accidental pressure increase.

Whenever under operation, the setup is surrounded by a box made out of thick and hard plywood. The area surrounding the box is protected by walls in every direction so that even if something did break, nothing solid should fly too far or with velocities too high. The gas cylinders are behind one of these walls, which makes them safely accessible and separated from the measurement area. The gas lines are equipped with safety cables, which are attached from both ends. The room is closed off so that people cannot accidentally walk in.

The setup operator wears hearing protection at all times, along with a protective mask. The valves on the vessel along with the quick-connect need to be operated manually, and thick gloves are used whenever this needs to be done. Both the thermocouple and the pressure transmitter have their connectors outside the plywood box so that they can be safely disconnected.

As almost all connections in the setup are done with thread connections, it is relatively easy to see if the connections have started to open. All the valves are lined horizontally so that if any of the connectors were to loosen, the valves would not match up any more. No safety valve or relief valve is present in the system. There is no heating inside the vessel and it should not be possible for any chemical reactions such as combustion to take place inside the vessel, so the only pressure increase to the system comes from the gas cylinder. Only one gas cylinder is connected at any given time. The gas cylinders are controlled manually, which means that the pressure cannot increase without the operator increasing it from the cylinder regulator.

When operating at pressures higher than 15 bar, the root valve right after the pressure regulator is closed whenever the pressure is not currently being increased, which would cover roughly 95% of the time. This limits the potential amount of released gas in case of a break to what is currently inside the setup. The room is well ventilated, and any gas vented from the setup due to evacuating the line for disconnecting the quick-connect or emptying the vessel at the end of the run, is vented outside the building.

4.2 Sample preparation

Carbon-based materials were chosen to be used as adsorbents in this work. The carbon samples were produced both in a muffle furnace and in a bubbling fluidized

bed reactor (BFB). Some samples were only carbonized, others were chemically treated prior to the heat treatment to produce activated carbons. Commercial granular activated carbon provided by Chemviron with product code F200, typically used for water purification, was used as comparison.

Norway spruce was chosen as the precursor material for the activated carbon. The precursor material used was sawn in the shape of small cubes with an approximate side length of 7 mm. Some of these cubes were directly carbonized, some were chemically activated prior to it, as seen in table 4.2.

Typical composition of Norway spruce can be seen in table 4.1. The values shown are for stem wood, out of which the samples were made. Bark, branches and other parts of the tree typically have different compositions. Suhas et al. suggest that lignin is the most important component when making activated carbons from lignocellulosic materials, with ligning providing a better char yield and microporosity than the other components [67].

Table 4.1: Typical chemical composition of Norway spruce [64].

Component	Median amount	
Cellulose	42.0	%
Hemicelluloses	26.6	%
Lignin	27.4	%
Extractives	2.0	%

A large number of samples were prepared, but only the ones seen in table 4.2 were measured with the setup due to time limitations. The first letter defines the heating method: M stands for muffle furnace and B for the BFB. Next number, here 500, refers to the heating temperature in degrees Celcius. The letter A means that an activating agent was used and the number following it is the impregnation ratio. An impregnation ratio designated as 1 meaning equal mass ratios of wood and phosphoric acid and 05 meaning 0.5 g of H_3PO_4 per one gram of wood.

Table 4.2: Prepared carbon samples.

Sample name	Temperature [°C]	Heating rate [°C/min]	Activation method
M500	500	7	-
M500A05	500	7	0.5 g H_3PO_4/1 g wood
M500A1	500	7	1.0 g H_3PO_4/1 g wood
B500	500	6000	-

4.2.1 Chemical activation

Some of the samples were chemically activated with phosphoric acid. A ratio of 1 g of H_3PO_4 per gram of wood was chosen to maximize the micropore volume according to [32]. The phosphoric acid was diluted with distilled water from the orignilal concentration of 85 % to approximately 42.5 % to completely submerge the wood cubes in the solution. The impregnation was performed in a 1 l glass bottle that was shaken regularily through the impregnation. The samples were kept in an oven at 85 °C for 6 hours to allow complete impregnation and then at 105 °C for 16 hours to remove excess moisture.

After carbonization the activated samples were washed with boiling distilled water until a pH of approximately 6 was reached. Then the samples were dried in 105 °C for 16 hours, after which they were weighted.

The first few activated batches were really poorly impregnated, including sample M500A05. This batch was prepared with only 0.5 g of activating agent per gram of precursor material. The last, succesful batch of cubes, M500A1, turned completely black after the impregnetion and drying. This was tested by crushing multiple sample cubes. The cubes in the former sample batch were only partially blackened, clearly indicating that the phosphoric acid had not impregnated the cubes properly. This may have been due to the lower acid amount, lower amount of solution, less shaking and performing the impregnation in ambient temperature instead of an oven. The cubes were still dried similarily to the properly activated sample.

4.2.2 Carbonization

Carbonization was conducted under nitrogen flow in either a muffle furnace or a bubbling fluidized bed reactor.

The muffle furnace is a small and old ceramic oven as shown in figure 4.3. The sample is loaded into the furnace from the front door seen left in the figure. Samples are kept in small crucibles and two of them can fit inside the furnace at a time. The samples are subjected to nitrogen flow to remove excess air from them before they are set into the crucibles and covered with a lid.

In the middle of the furnace door is a 5 cm x 3 cm hole that is covered with high-temperature insulation wool. Two small holes are made into the wool so that a K-type thermocouple and a nitrogen injection pipe can be lead inside the furnace. The nitrogen comes from a cylinder and the flow is set to the smalles possible flow that can be achieved. The furnace has no pre-made route for the exiting exhaust gases, so they leak from the two holes and from the sides of the furnace door. An

exhaust hood was used to collect the gases and the room ventilation was set to the highest level attainable.

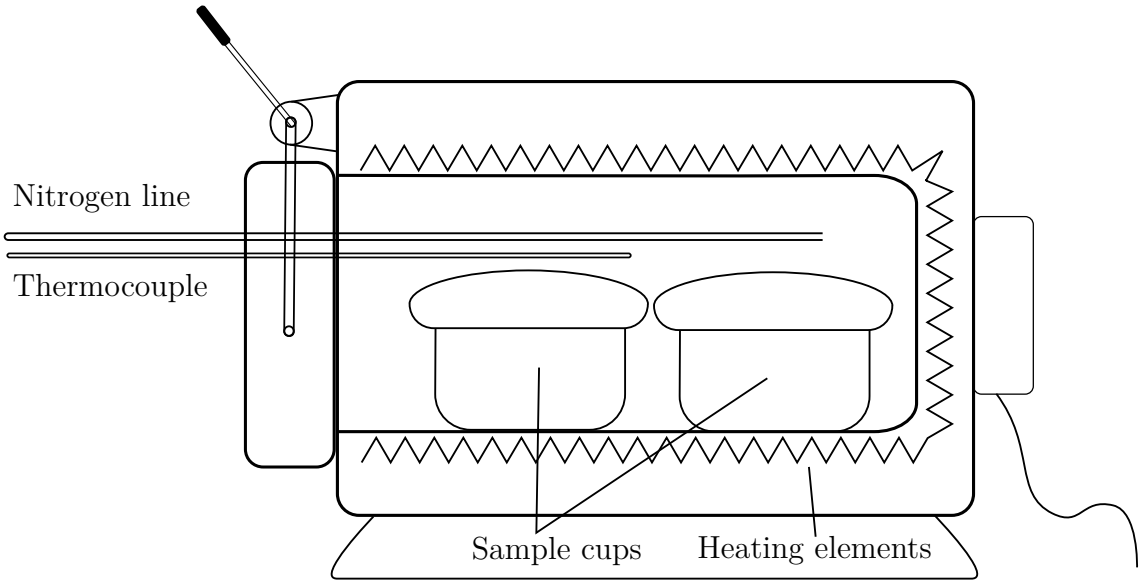

Figure 4.3: Muffle furnace.

The heating rate and the temperature of the furnace needed to be controlled manually. A voltage transformer was used to adjust the input voltage and the temperature inside was measured with the thermocouple seen in figure 4.3. The temperature was measured every 10 seconds and the temperature curve was plotted on the PC screen. By regularily increasing the voltage from the transformer, it was attempted to keep a relatively constant heating rate of 5-10 °C/min. The heating curves of the samples prepared in the muffle furnace can be seen in figure 4.4. Slight problems came from the positioning of the thermocouple: If the thermocouple was too close to the end of the nitrogen line, the nitrogen flow would cool the thermocouple down. If the feed line was placed as far as possible, the flowing gas had time to warm up and the thermocouple placed halfway in the oven registered a temperature closer to the real value. Relatively similar heating rates were achieved no matter where the thermocouple was, but the absolute temperature recorded varied by dozens of degrees. Maintaining a constant temperature of 500 °C proved to be difficult due to the slow temperature response of the system. Whenever the temperature exceeded 500 °C, the nitrogen flow was temporarily increased to lower the temperature.

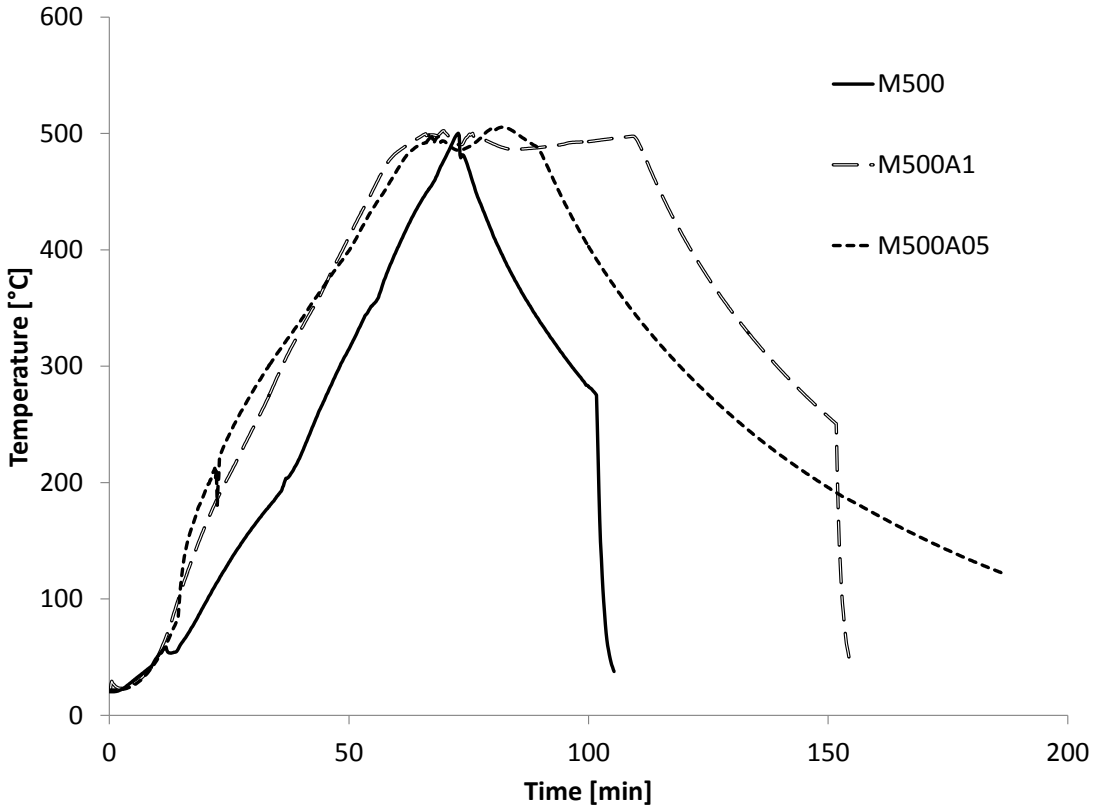

Figure 4.4: Heating curves for samples M500, M500A1 and M500A05.

Bubbling fluidized bed reactor consists of a steel tube surrounded with heating elements. The reactor can be seen in figure 4.5.

The reactor pipe is 1000 mm long and has a diameter of 90 mm. The heating elements cover 700 mm of the pipe length. Pressurized, preheated gas enters the tube from the bottom and flows up through the tube, exiting from the top to the exhaust hood. The gas flows through the fluidization sand above the adjustable grate. With sufficient gas velocities the sand becomes suspended and starts to behave in a fluid-like manner, greatly increasing the heat transfer rate inside the reactor. The gas is fed from a cylinder and the flow velocity is set manually to a suitable level. The preheater is 20 cm long metal tube with an electric heater and a K-type thermocouple in it. The preheater is controlled manually with a voltage transformer by observing the measured temperature and adjusting the power accordingly. The reactor has a thermostat control where a set point can be given. The temperature of the preheated gas is set to approximately the same as the desired reactor temperature, rather smaller than larger than the set point of the thermostat.

A sample basket made out of stainless steel can be lowered into the reactor from the top. The basket is equipped with a K-type thermocouple to measure the temperature that the samples experience. Another K-type thermocouple is used to control the

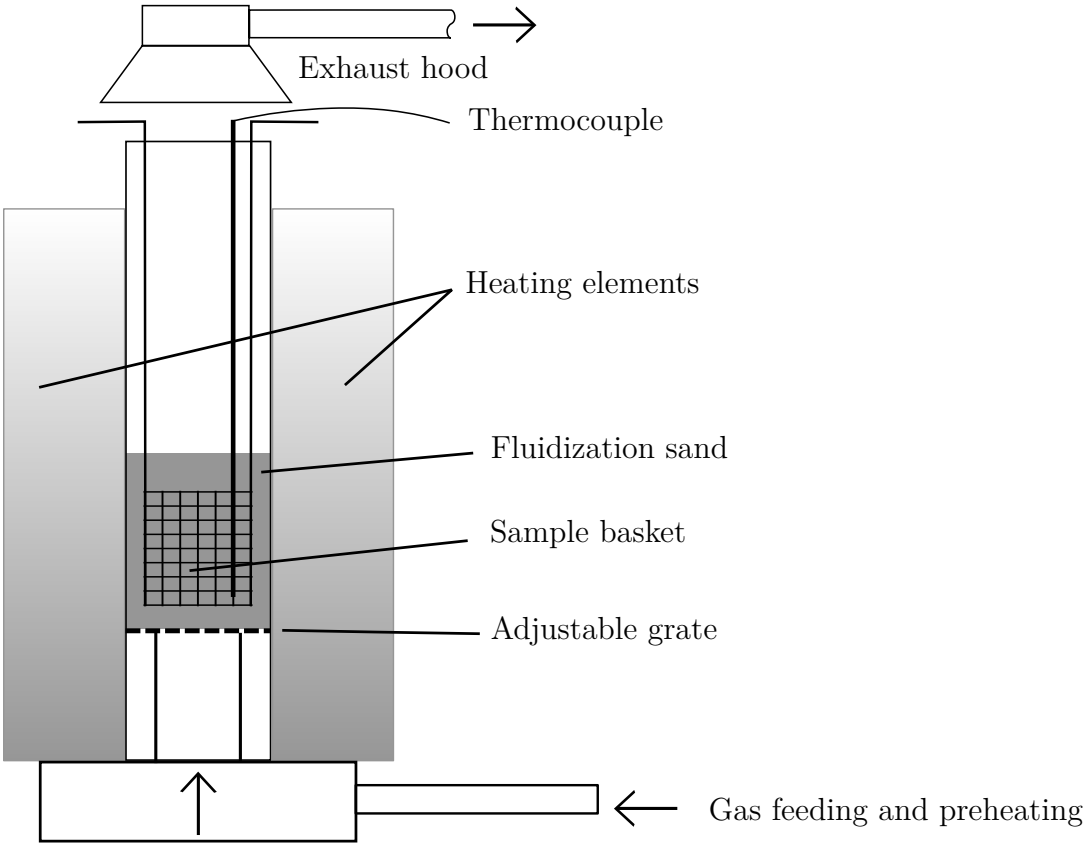

Figure 4.5: Bubbling fluidized bed reactor.

reactor temperature. The heat transfer coefficient inside the reactor was calculated from an implicit heat transfer model in MATLAB. The model was validated by inserting a spherical steel ball with a thermocouple inside it to the reactor and measuring the temperature response. As the heat conductivity of the steel ball and the temperature increase rate inside it were known, the only unknown variable was the heat transfer coefficient in the bed. Another measurement should have been done with the steel ball thermocouple inside the sample basket to see its effect on the heating rate.

The heating curve for sample B500 can be seen in figure 4.6. The wood cubes were kept in the reactor until the temperature reached 500 °C and no visible gases were released anymore. Then the sample basket was lifted from the reactor and submerged into liquid nitrogen several times, until the boiling of the liquid calmed down.

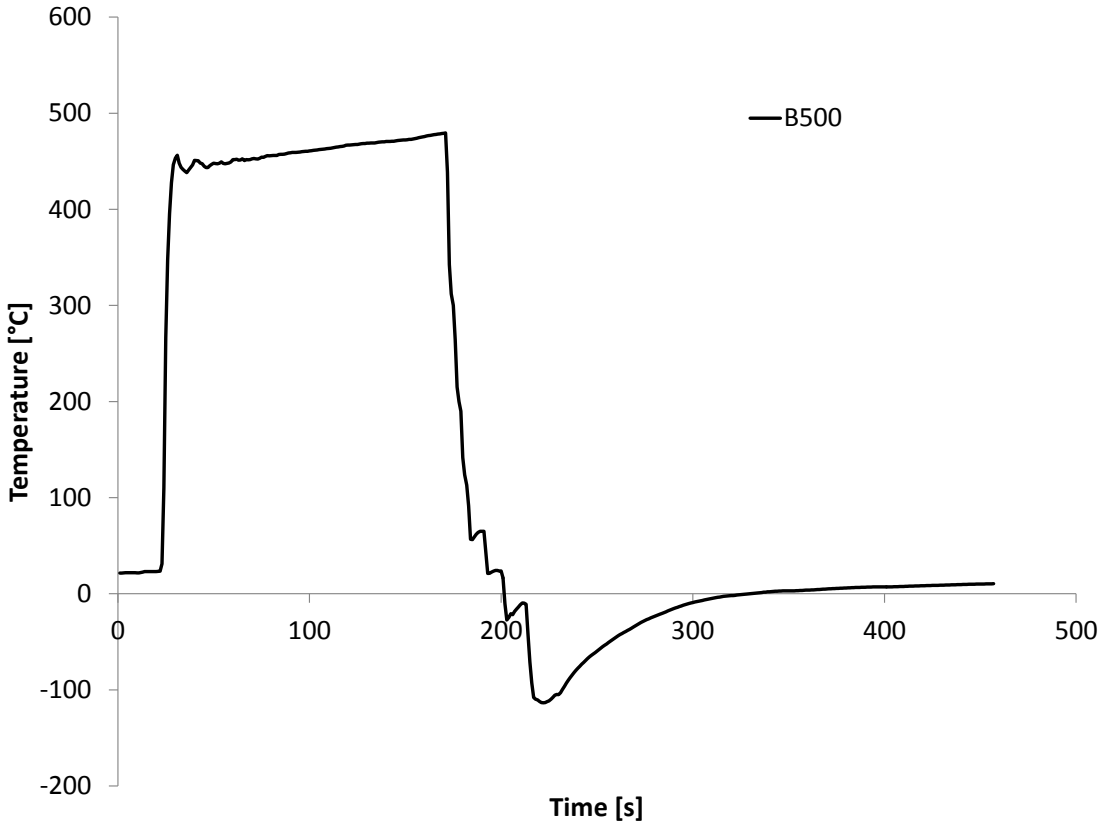

Figure 4.6: Heating curve for sample B500.

4.2.3 Sample degassing

Prior to the measurements, the samples need to be degassed. After the carbonization the samples are kept in plastic, closed sample cups with some leftover air in them. Air gases and water vapor adsorb on the surface of the sample, and these need to be removed so that the adsorption capacity of methane can be determined. This is done by heating the sample to a temperature of over 100 °C, then placing the sample in the pressure vessel and evacuating the vessel. The sample is allowed to cool down and the vacuum pump is kept running for some time. The pump is also used just prior to the measurements to remove any slowly desorbing gases or any possible air leakage from outside.

4.3 Measurement procedure

The helium measurements were conducted as follows:

1. The evacuated and sample filled vessel is weighed and the pressure and temperature are measured.

2. The gas line is purged with helium to remove excess air from it. Then the line is connected to the vessel.
3. The pressure is increased to 5 bar(a).
4. All lines are disconnected. Weight is measured.
5. The cables for pressure and temperature are connected and they are measured.
6. The gas line is reconnected. The pressure is increased as high as the helium cylinder regulator allows, approximately 10 bar(a).
7. Same as steps 4 and 5.
8. The cylinder regulator is closed. The pressure from the vessel and the line are released. The vessel is evacuated with the vacuum pump.

Measurements in intermediate pressures between 0 and 10 bar(a) can be made, but only the last measurement is used for the calculation of the void volume.

Similar procedure is followed with methane, with some exceptions:

1. The evacuated and sample filled vessel is weighed and the pressure and temperature are measured.
2. The gas line is purged with methane to remove traces of other gases. Then the line is connected to the vessel.
3. The pressure is increased to a desired level. The root valve is closed.
4. The gas line is depressurized.
5. All lines are disconnected. Weight is measured. The cables for pressure and temperature are connected.
6. The temperature and the pressure are allowed to stabilize, then they are measured.
7. The gas line is reconnected.
8. Steps 3-7 are repeated with desired pressure increase intervals until the desired maximum pressure is reached.
9. The cylinder regulator is closed. The pressure from the vessel and the line are released.

The pressure increase interval can be anything from 1 bar to 15 bar, depending on the pressure level. At lower pressures, a smaller interval can be used more easily. At higher pressures, however, there is hardly any reason to have too small an interval as this provides little additional information.

The ambient temperature and humidity were not necessarily constant during and between measurement, nor was the temperature of the vessel due to the changes in its internal pressure and the adsorption/desorption enthalpy changes. Therefore the scale was calibrated before each run to ensure accuracy. The void volume of the container is calculated from the helium measurement.

4.4 Data handling

The void volume is determined from the helium measurements as explained in chapter 3.4.6 and it is used to calculate the methane uptake in a case where no adsorption takes place. The uptake is calculated from the equation 3.15 in every measured temperature and pressure. The Z-factor is calculated by solving the equation 3.22 in every used temperature and pressure. Three curves are made for the methane reference uptake: the calculated methane uptake along with upper and lower error limits. The minimum-maximum method is used to determine the propagation of uncertainty. That is, the nominal uptake is calculated normally but the error limits are calculated by using the minimum and maximum of the measured values to calculate the smallest and largest possible result. Uncertainty is assumed to be ± 0.01 g for the scale, ± 0.25 bar for the pressure transmitter, and ± 2.2 °C for the thermocouple. Matlab is used for all the calculations.

5. RESULTS

5.1 Carbonized samples

The mass loss of the prepared carbon samples can be seen in table 5.1. The initial mass of the raw material could not be measured for the activated samples, as the activation was done in larger batches but only a part of the chemically treated material was actually carbonized.

The sample B500 carbonized in the BFB had some sand attached to the cubes during the carbonization process. This sand could not be removed without destroying the samples. Therefore the true mass loss is even greater than the 80 % shown in the table. There is also a chance that some of the cubes were lost in the process of carbonization if some of the cubes were thrown away from the sample basket due to the movement of the gas and the fluidization sand. If some of the cubes broke down due to their movement in the basket, the parts might have been small enough to fall through the holes of the basket.

The amount of the carbon prepared varies greatly between the sample types. The commercial carbon F200 was readily available and a full sample cup, approximately 59 g, was used for the measurements. For the other samples, the initial mass is the largest amount that could be carbonized at a time. Multiple batches could have been made of each sample, but this was not considered necessary at the time the samples were prepared.

Table 5.1: Carbon samples.

	Mass [g]			
	Prior to carbonization		Final mass	Mass loss [%]
Sample	Raw material	With chemicals		
M500	26.02	-	7.43	71.4
M500A05	-	31.81	15.52	51.2
M500A1	-	61.10	14.63	76.0
B500	32.16	-	6.42	80.0
F200	-	-	58.84	-

5.2 Measurement results

Methane adsorption on five carbon samples was studied. Measurement runs for the samples M500, B500 and M500A05 can be seen in figures 5.1-5.3.

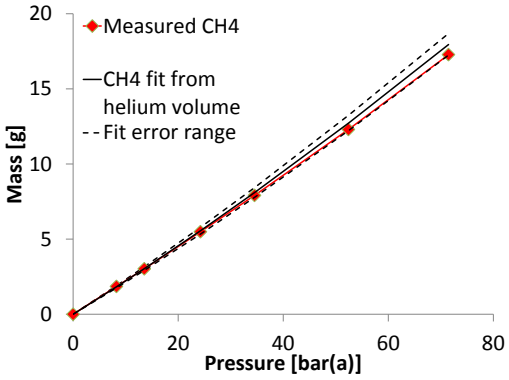

Figure 5.1: Measured values and reference line for M500.

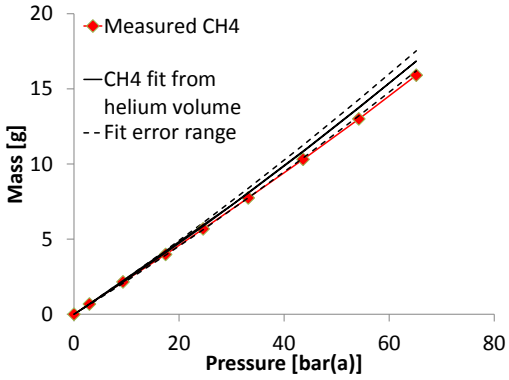

Figure 5.2: Measured values and reference line for B500.

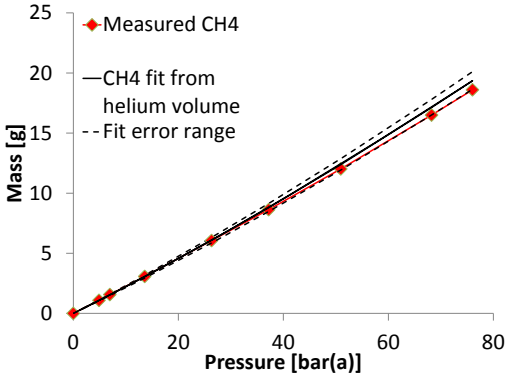

Figure 5.3: Measured values and reference line for M500A05.

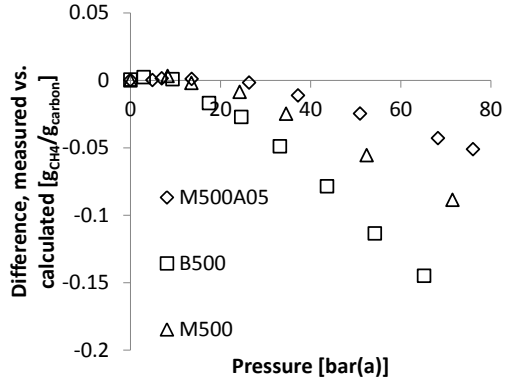

Figure 5.4: Calculated values deducted from the measured values, per one gram of carbon.

The measured values are shown with the squares. The solid black line is the reference curve, or how much methane the void space could hold if no wall effects take place. The dashed lines are the calculated error ranges for the reference line. As it can be seen, the measured values follow roughly the lower error line and in figure 5.2 even going below it. This means that any adsorption taking place is indistinguishable due to the error margins. This could be due to either the sample size being too small or just that there is not enough adsorption taking place for it to be noticeable.

In figure 5.4 the reference values are deducted from the measured values and then divided by the sample amount. This difference would be the excess adsorption if the values were positive. The negative values, however, can most likely be explained both by the uncertainty of the setup and the larger void space seen by helium than

by methane. As can be assumed by observing the figures 5.1-5.3, the uncertainy ranges in figure 5.4 are high.

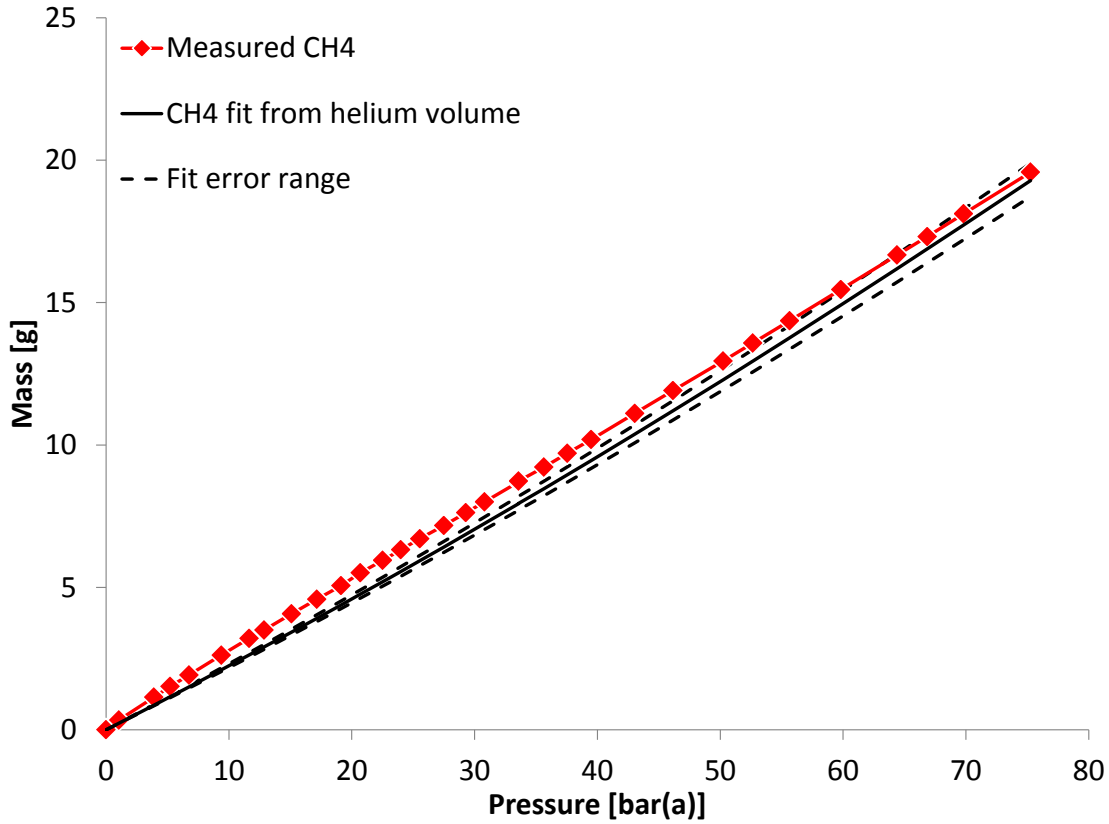

Figure 5.5: Measured values and reference line for M500A1.

The sample M500A1 seen in the figure 5.5 look much more promising than the previous samples. The measured values are at all points above the reference curve and intersecting the upper error range only at very high pressures. The difference between the measured values and the reference curve is rather small. There clearly is a significant amount of adsorption present, but the sample amount is too small for its accurate determination. This can be seen in figure 5.6 which shows the adsorbed amount in grams per gram of carbon. The values are predominantly positive, but the error ranges spread rapidly with the lower error range even going negative. At 75 bar(a) the adsorbed amount is 0.02 g_{CH4}/g_{carbon} and has uncertainty of ± 0.04 g_{CH4}/g_{carbon}. Maximal adsorption capacity is reached around 20 bar(a) but the storage capacity does not stop increasing there. After the maximum, the curve starts to decline and converge towards a situation that could be reached purely with compression. The curve resembles the excess adsorption curve seen in figure 3.3.

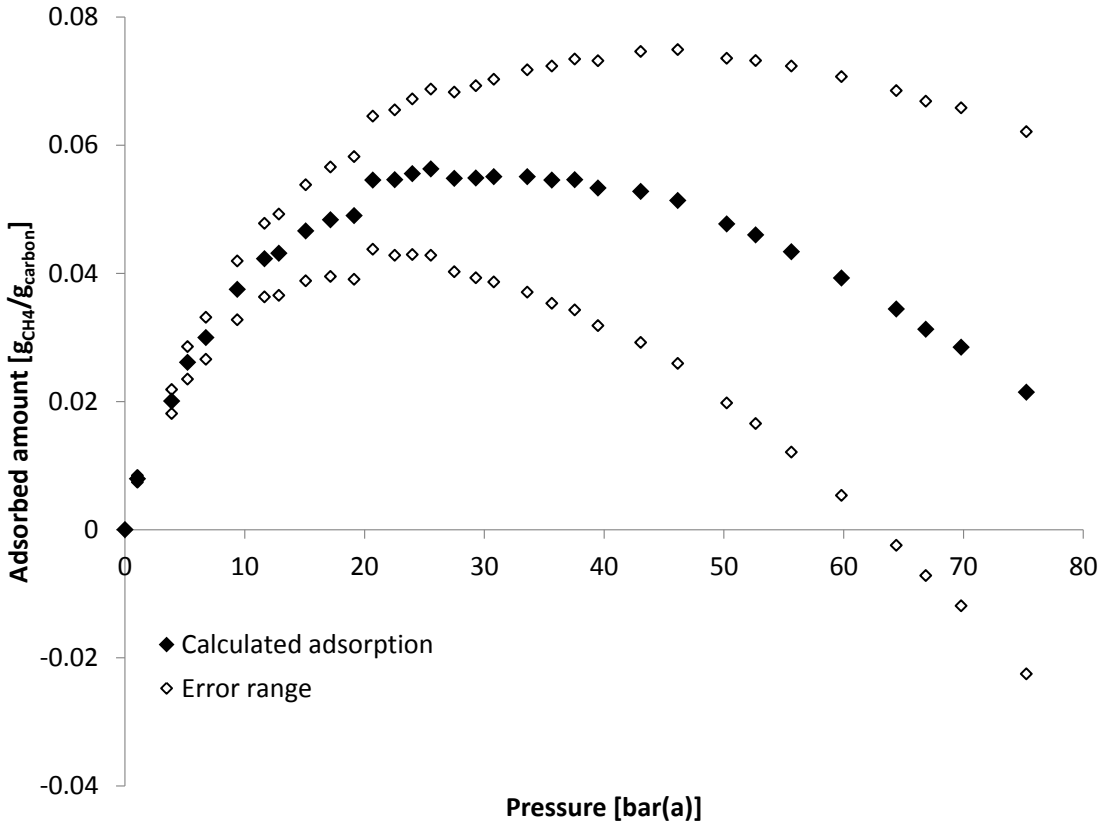

Figure 5.6: Excess adsorption of CH_4 on sample M500A1.

The measured values for the commercial F200 activated carbon, seen in figure 5.7, are clearly the best of the measurement runs. With a sample size that is almost four times greater than that of the two next largest samples and approximately eight times greater than the smallest samples, the measured values are clearly above the reference curve. This has the advantage of providing much smaller uncertainty limits as seen in figure 5.8 compared to the limits in 5.6.

Despite the adsorption in figure 5.7 looking greater than that of figure 5.5, the adsorbed amount per mass of adsorbent is slightly lower for F200 than it is for M500A1. This can be seen by comparing the figures 5.6 and 5.8. F200 is designed for water purification, so it is no surprise that an adsorbet specifically prepared for methane storage can reach higher storage values. Interestingly the decline in the excess adsorption of M500A1 is much higher than it is for F200. Again, this might be due to the high uncertainty caused by the low sample amount.

Unfortunately the specific surface area for sample M500A1 could not be determined due to budget limitations, so no comparison can be made between the two samples other than the adsorption values. The process for preparing sample M500A1 is far from optimized. Even though the sample was prepared following directions given in

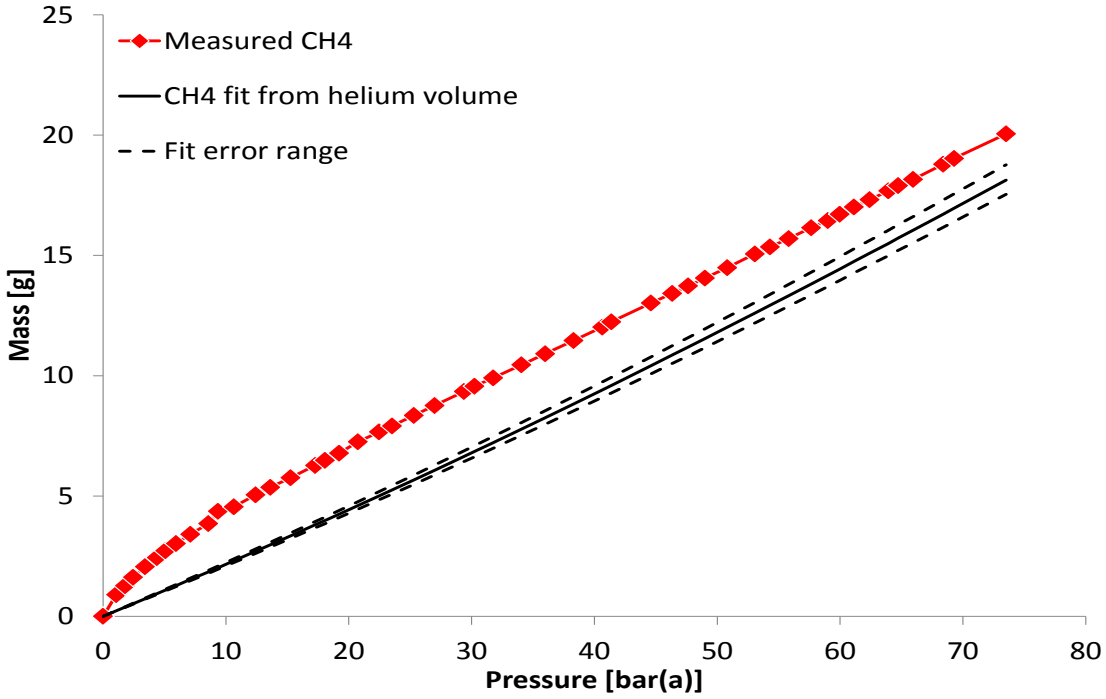

Figure 5.7: Measured values and reference line for F200.

[32], the inexperience in the preparation of activated carbons may have significantly lowered the adsorption potential of the sample.

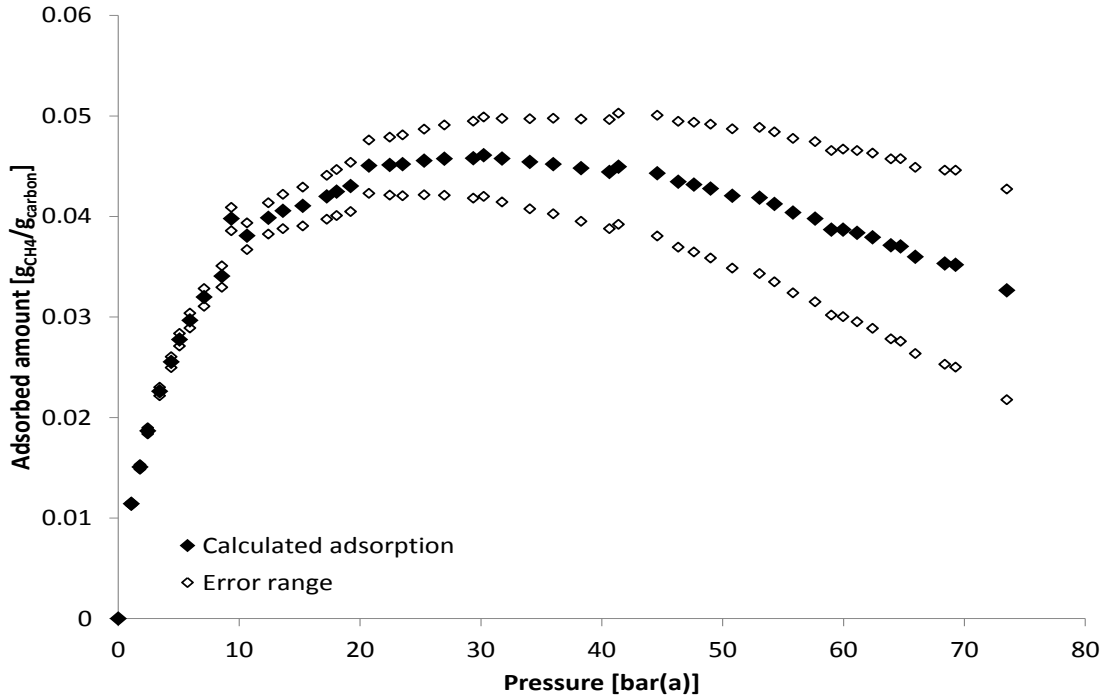

Figure 5.8: Excess adsorption of CH_4 on sample F200.

5.3 Discussion

The setup itself was tested by measuring the density of a block of aluminum. The measured result was within 2 % of the real density of the material. The thermocouple, the pressure transmitter and the balance are all new and therefore should have no problems with aging. They were not tested or calibrated individually in any way to test their zero points or linearity. The pressure achieved by evacuating the vessel was assumed to be 0 bar(a), as no better knowledge was available. Attaching another transmitter with a lower pressure range could greatly increase the accuracy of both the vacuum pressure determination and the determination of the void volume.

Other sources of error may include failing to account for some physical factor. The results show that adsorption takes place in some of the samples and no adsorption can be seen in samples with little surface area such as on a solid aluminum block. The temperature was kept relatively isothermal. The little variations in the temperature during and between measurements may affect the adsorption isotherms, but there is no knowledge as to the magnitude of the effect.

The effect of degassing of the samples needs to be studied further. The current procedure might not be able to release all the gases and water vapor adsorbed on the sample, thus lower the adsorption potential for methane and giving a larger error due to the different size and mass of nitrogen molecules compared to methane.

The size of the cubes is relatively large. It was feared that if the samples were ground to dust prior to the heating, the wood particles might burn too easily due to the large surface area of the particles and due to the extra oxygen trapped between the particles. The high surface area compared to the amount of gases released could also lead to increased gasification due to self-gasification, leading to a much lower yield. The cubes could have been ground after the heating, but it was chosen to test them as they are and grind further samples for comparison. One problem that may arise from the large size of the cubes is that they might have closed or ink-bottle pores that are accessible to helium but not methane. Grinding the samples could open these pores.

Increasing the number of measurements per sample might help to account for variance in the measurements. Measurement runs took a lot of time and thus only one run was made per sample. The most critical measurement is the helium volume determination, and doing it multiple times might help with the accuracy. A cylinder regulator for helium with a higher operating pressure would significantly increase the accuracy.

Too small amounts of each of the carbon samples were produced. Both the muffle furnace and the sample basket for the BFB were fully loaded with the wood cubes

when the carbonizing was done, but multiple batches should have been produced. With a sample size closer to the approximately 60 g used with the commercial activated carbon F200, the adsorption should be much more visible for samples with lower adsorptive capabilities. The setup could be used with much higher amounts, even sample sizes above 100 g should be measurable. A minimum sample amount of 50 g is suggested for future measurements.

Calculating the total adsorption, instead of the excess adsortion, from the current measurements would require the determination of both the skeletal and the bulk density of the sample. The former can be calculated with some degree of accuracy from the void volume measurements performed, but determining the bulk density of the materials is more difficult. The measured samples would need to be grinded and compressed to measure the bulk density and the adsorption measurements would need to be performed to the compressed sample, as the specific surface area may differ greatly between the powdered and the compressed form. For the sake of getting an estimate on the volumetric uptake of the sample M500A1, its bulk density is assumed to be 0.5 g/cm^3 which gives an uptake of approximately 70 V_{CH4}/V_{carbon} at 35 bar(a) and 22 °C. [68]

5.4 Suggestions for future

The setup could be relatively easily changed to a volumetric adsorption setup. This would require an additional pressure vessel which could prove to be expensive, but would most likely greatly increase the accuracy of the measurements. This would allow the usage of a temperature regulated bath to keep the sample vessel isothermal and to test adsorption behavior in different temperatures.

Some characterization could be done to the more promising samples. Determination of skeletal and bulk density, specific surface area and porosity distribution would give important knowledge on the properties of the samples. No equipment for this is currently available, which means it would need to be done by a third party.

Future research should focus on producing efficient adsorbents as economically as possible. The effect of the carbonization temperature, heating rate, and the duration of the thermal treatment on the development of the surface area and porosity distribution should be studied. As can be seen from the prepared samples, heat treatment alone does not seem to be enough for for the production of efficient adsorbents and some form of activation will be required. Carbon aquired from the decomposition of methane and from the production of pyrolysis oil should be studied. These carbons are treated only with heat and therefore are unlikely to directly be good adsorbents. The effect of activating them and the possibility of integrating the activation step

to their production need to be studied. The porosity reduction due to the deformation of the ash content in high temperatures may limit the maximum carbonization temperature, but this needs to be studied further [21].

It needs to be remebered that adsorption storage of methane and natural gas are two different things. This can especially be seen in repeated adsorption/desorption cycles which were not performed in these measurements. No measurements were conducted with CO_2, even though its storage is of much interest. Storage of hydrogen can most likely not be measured with the current setup due to its low molecular weight compared to the precision of the balance. Selectivity, enthalpy change and rate of adsorption can not be currently measured and modifying the setup to include them does not seem feasible.

6. CONCLUSIONS

An experimental setup for measuring the gas uptake of microporous solids was constructed to study their use as adsorption storage of gases. The measurements were conducted with self prepared carbon samples and with a commercial activated carbon. Measurements were made with methane to simulate the storage of natural gas.

It was shown that the setup could be used in the adsorption study of materials. The setup is far from optimal, as the precision is orders of magnitude lower than that of commercial adsorption measurement devices. Most of the problems were caused by time constraints and delays in the construction of the setup. Sample size requirement for measurements are accordingly much higher. A minimum sample size of 50 g is recommended for accurate measurements. However, the setup provides a relatively cheap and easy way to characterize materials. Functionality and limitations of the setup were determined and insight gained for future development of the setup. In hindsight, a purely volumetric apparatus would have been better in almost every aspect. It would have, however, required an additional pressure vessel which was not available at the time of construction.

The constructed setup should provide easy means to determine if a material can be used as an adsorbent. For laboratory scale experimentation it should fulfill its role of providing initial information on materials. The samples prepared for this work are not feasible for real applications, but they were useful in testing the setup and providing insight into the preparation of further samples. An excess adsorption value of approximately 0.05 ± 0.02 g_{CH4}/g_{carbon} in 35 bar(a) and 22 °C was aquired for the best prepared sample, which equals approximately 70 cm^3 of methane in 1 cm^3 of carbon if the carbon bulk density is assumed to be 0.5 g/cm^3. This is twice the uptake of CNG storage in the same pressure and 11 % of the energy density of LNG. The measurements of the other samples showed that thermal treatment alone does not seem to be sufficient for the prepararation of useful adsorbents from wood.

Adsorption storage technology is currently not broadly used but it has the potential to be feasible in the future. Its passive nature, advances in material studies and changes in global energy and emission prices will likely work as the driving force in the adoption of adsorption technology in gas storage applications.

REFERENCES

[1] Alonso-Vicario, A., Ochoa-Gómez, J. R., Gil-Río, S., Gómez-Jiménez-Aberasturi, O., Ramírez-López, C., Torrecilla-Soria, J., and Domínguez, A. Purification and upgrading of biogas by pressure swing adsorption on synthetic and natural zeolites. *Microporous and Mesoporous Materials 134*, 1-3 (2010), 100 – 107.

[2] Antoniou, M. K., Diamanti, E. K., Enotiadis, A., Policicchio, A., Dimos, K., Ciuchi, F., Maccallini, E., Gournis, D., and Agostino, R. G. Methane storage in zeolite-like carbon materials. *Microporous and Mesoporous Materials 188* (2014), 16–22.

[3] Bartell, F. E., Thomas, T. L., and Fu, Y. Thermodynamics of adsorption from solutions. iv. temperature dependence of adsorption. *The Journal of Physical Chemistry 55*, 9 (1951), 1456–1462.

[4] Bhatnagar, A., Hogland, W., Marques, M., and Sillanpää, M. An overview of the modification methods of activated carbon for its water treatment applications. *Chemical Engineering Journal 219*, 0 (2013), 499 – 511.

[5] Bond, D. C. Underground storage of natural gas. Illinois State Geological Survey, 1975.

[6] British Petroleum. Statistical review of world energy 2014, 2014.

[7] Brunauer, S., Emmett, P. H., and Teller, E. Adsorption of gases in multimolecular layers. *Journal of the American Chemical Society 60*, 2 (1938), 309–319.

[8] Chang, C. Measuring density and porosity of grain kernels using a gas pycnometer. *Cereal Chem 65*, 1, 13–15.

[9] Chang, F., Zhou, J., Chen, P., Chen, Y., Jia, H., Saad, S. M., Gao, Y., Cao, X., and Zheng, T. Microporous and mesoporous materials for gas storage and separation: a review. *Asia-Pacific Journal of Chemical Engineering 8*, 4 (2013), 618–626.

[10] Choudhary, T. V., et al. Hydrogen production via catalytic decomposition of methane. *Journal of Catalysis 199*, 1 (2001), 9–18.

[11] Chue, K. T., Kim, J. N., Yoo, Y. J., Cho, S. H., and Yang, R. T. Comparison of activated carbon and zeolite 13X for CO_2 recovery from flue gas by pressure swing adsorption. *Industrial & Engineering Chemistry Research 34*, 2 (1995), 591–598.

[12] Cook, T., Komodromos, C., Quinn, D., and Ragan, S. Chapter 9 - adsorbent storage for natural gas vehicles. In *Carbon Materials for Advanced Technologies*, T. D. Burchell, Ed. Elsevier Science Ltd, Oxford, 1999, pp. 269 – 302.

[13] Cracknell, R. F., Gordon, P., and Gubbins, K. E. Influence of pore geometry on the design of microporous materials for methane storage. *The Journal of Physical Chemistry 97*, 2 (1993), 494–499.

[14] Dąbrowski, A. Adsorption - from theory to practice. *Advances in colloid and interface science 93*, 1 (2001), 135–224.

[15] DOE move program. Methane Opportunities for Vehicular Energy, Advanced Research Project Agency-Energy, U.S. Dept. of Energy, Funding Opportunity no. DE-FOA-0000672, 2012.

[16] Durr, C., Coyle, D., Hill, D., and Smith, S. LNG technology for the commercially minded. Gastech, 2005.

[17] El-Gohary, M. M. The future of natural gas as a fuel in marine gas turbine for lng carriers. *Proceedings of the Institution of Mechanical Engineers, Part M: Journal of Engineering for the Maritime Environment* (2012).

[18] Elam, C. C., Padró, C. E. G., Sandrock, G., Luzzi, A., Lindblad, P., and Hagen, E. F. Realizing the hydrogen future: the international energy agency's efforts to advance hydrogen energy technologies. *International Journal of Hydrogen Energy 28*, 6 (2003), 601–607.

[19] EU Commission. In-depth study of european energy security, commission staff working document, accompanying the document: European energy security strategy, 2014.

[20] Fager-Pintilä, M. Thermocatalytic decomposition of methane. Master's thesis, Tampere University of Technology, 2012.

[21] Fager-Pintilä, M. Thermocatalytic decomposition of methane: Annual report, 2013.

[22] Fagerlund, G. Determination of specific surface by the bet method. *Matériaux et Construction 6*, 3 (1973), 239–245.

[23] Farha, O. K., Eryazici, I., Jeong, N. C., Hauser, B. G., Wilmer, C. E., Sarjeant, A. A., Snurr, R. Q., Nguyen, S. T., Yazaydın, A. Ö., and Hupp, J. T. Metal-organic framework materials with ultrahigh surface areas: Is the sky the limit? *Journal of the American Chemical Society 134*, 36 (2012), 15016–15021. PMID: 22906112.

[24] Foo, K., and Hameed, B. Insights into the modeling of adsorption isotherm systems. *Chemical Engineering Journal 156*, 1 (2010), 2 – 10.

[25] Gasum. Porvoon tuotantolaitos. `http://www.gasum.fi/Tietoa_Gasumista/Skangass/Tuotantolaitokset/`. Accessed: 16.2.2015.

[26] Giesche, H. Mercury porosimetry: a general (practical) overview. *Particle & particle systems characterization 23*, 1 (2006), 9–19.

[27] Ha, N. L., Ungvarai, J., and Kovats, E. S. Adsorption isotherm at the liquid-solid interface and the interpretation of chromatographic data. *Analytical Chemistry 54*, 14 (1982), 2410–2421.

[28] Inagaki, M., and Kang, F. *Carbon Materials Science and Engineering: From Fundamentals to Applications*. Tsinghua University Press, 2006.

[29] International Energy Agency. Key world energy statistics, 2014.

[30] International Energy Agency and Organisation for Economic Co-operation and Development. *World Energy Outlook 2009*. WORLD ENERGY OUTLOOK. OECD/IEA, 2009.

[31] Ioannidou, O., and Zabaniotou, A. Agricultural residues as precursors for activated carbon production – a review. *Renewable and Sustainable Energy Reviews 11*, 9 (2007), 1966 – 2005.

[32] Jagtoyen, M., and Derbyshire, F. Activated carbons from yellow poplar and white oak by H_3PO_4 activation. *Carbon 36*, 7 - 8 (1998), 1085 – 1097.

[33] Jänchen, J., Ackermann, D., Stach, H., and Brösicke, W. Studies of the water adsorption on zeolites and modified mesoporous materials for seasonal storage of solar heat. *Solar Energy 76*, 1-3 (2004), 339 – 344. Solar World Congress 2001.

[34] Jaramillo, P., Griffin, W. M., and Matthews, H. S. Comparative life-cycle air emissions of coal, domestic natural gas, LNG, and SNG for electricity generation. *Environmental Science & Technology 41*, 17 (2007), 6290–6296.

[35] Judd, R., Gladding, D., Hodrien, R., Bates, D., Ingram, J., and Allen, M. The use of adsorbed natural gas technology for large scale storage.

[36] Kadirvelu, K., Kavipriya, M., Karthika, C., Radhika, M., Vennilamani, N., and Pattabhi, S. Utilization of various agricultural wastes for activated carbon preparation and application for the removal of dyes and metal ions from aqueous solutions. *Bioresource technology 87*, 1 (2003), 129–132.

[37] Keller, J. U., and Staudt, R. *Gas Adsorption Equilibria*. Springer US, 2005.

[38] Keyaerts, N., Hallack, M., Glachant, J.-M., and D'haeseleer, W. Gas balancing rules must take into account the trade-off between offering pipeline transport and pipeline flexibility in liberalized gas markets.

[39] Kikkinides, E. S., Yang, R. T., and Cho, S. H. Concentration and recovery of carbon dioxide from flue gas by pressure swing adsorption. *Industrial & Engineering Chemistry Research 32*, 11 (1993), 2714–2720.

[40] Lowell, S., Shields, J., Thomas, M., and Thommes, M. Surface area analysis from the langmuir and bet theories. In *Characterization of Porous Solids and Powders: Surface Area, Pore Size and Density*, vol. 16 of *Particle Technology Series*. Springer Netherlands, 2004, pp. 58–81.

[41] Lozano-Castelló, D., Cazorla-Amorós, D., Linares-Solano, A., and Quinn, D. Activated carbon monoliths for methane storage: influence of binder. *Carbon 40*, 15 (2002), 2817 – 2825.

[42] Lozano-Castelló, D., Cazorla-Amorós, D., Linares-Solano, A., and Quinn, D. Influence of pore size distribution on methane storage at relatively low pressure: preparation of activated carbon with optimum pore size. *Carbon 40*, 7 (2002), 989 – 1002.

[43] Ma, S., and Zhou, H.-C. Gas storage in porous metal-organic frameworks for clean energy applications. *Chem. Commun. 46* (2010), 44–53.

[44] Martin, R. Adsorption of solutes at the liquid-gas interface as measured by gas chromatography and gibbs equation. *Analytical Chemistry 35*, 1 (1963), 116–117.

[45] Mason, J., Veenstra, M., and Long, J. Evaluating metal-organic frameworks for natural gas storage. *Chemical Science 5*, 1 (2014), 32–51. cited By 0.

[46] Mcnaught, A. D., and Wilkinson, A. *IUPAC. Compendium of Chemical Terminology, 2nd ed. (the "Gold Book").* Blackwell Scientific Publications; 2nd Revised edition edition, Aug. 1997.

[47] Mcnaught, A. D., and Wilkinson, A. *IUPAC. Compendium of Chemical Terminology, 2nd ed. (the "Gold Book").* Blackwell Scientific Publications; 2nd Revised edition edition, Aug. 1997.

[48] Menon, V., and Komarneni, S. Porous adsorbents for vehicular natural gas storage: a review. *Journal of Porous Materials 5*, 1 (1998), 43–58.

[49] Morris, R. E., and Wheatley, P. S. Gas storage in nanoporous materials. *Angewandte Chemie International Edition 47*, 27 (2008), 4966–4981.

[50] Myers, A. L., and Monson, P. A. Physical adsorption of gases: the case for absolute adsorption as the basis for thermodynamic analysis. *Adsorption 20*, 4 (2014), 591–622.

[51] National Renewable Energy Laboratory. Energy analysis: Biogas potential in the United States, 2013.

[52] NGVA Europe, and GVR. NGVs and fuel consumption worldwide, 2013.

[53] NGVA Europe, and GVR. Worldwide NGV shares in total vehicle market, 2013.

[54] Nijboer, M. The contribution of natural gas vehicle to sustainable transport. OECD Publishing, 2010.

[55] Peng, D.-Y., and Robinson, D. B. A new two-constant equation of state. *Industrial & Engineering Chemistry Fundamentals 15*, 1 (1976), 59–64.

[56] Radlinski, A., Mastalerz, M., Hinde, A., Hainbuchner, M., Rauch, H., Baron, M., Lin, J., Fan, L., and Thiyagarajan, P. Application of saxs and sans in evaluation of porosity, pore size distribution and surface area of coal. *International Journal of Coal Geology 59*, 3 (2004), 245–271.

[57] Ramos-Fernández, J. M., Martínez-Escandell, M., and Rodríguez-Reinoso, F. Production of binderless activated carbon monoliths by KOH activation of carbon mesophase materials. *Carbon 46*, 2 (2008), 384–386.

[58] Ross, S., and Chen, E. S. Adsorption and thermodynamics at the liquid-liquid interface. *Industrial & Engineering Chemistry 57*, 7 (1965), 40–52.

[59] Rouquerol, J., Avnir, D., Fairbridge, C. W., et al. Recommendations for the characterization of porous solids (technical report). *Pure and Applied Chemistry 66*, 8 (2009), 1739–1758.

[60] Ruthven, D. *Principles of Adsorption and Adsorption Processes*. Wiley-Interscience publication. Wiley, 1984.

[61] Sapag, K., Vallone, A., Blanco, A. G., and Solar, C. *Adsorption of Methane in Porous Materials as the Basis for the Storage of Natural Gas, Natural Gas*. InTech, http://www.intechopen.com/books/natural-gas/adsorption-of-methane-in-porous-materials-as-the-basis-for-the-storage-of-natural-gas, 2010.

[62] Sing, K. S. W., Everett, D. H., Haul, R. A. W., Moscou, L., Pierotti, R. A., Rouquerol, J., and Siemieniewska, T. Reporting physisorption data for gas/solid systems with special reference to the determination of surface area and porosity. *Pure and Applied Chemistry 57*, 4 (1985), 603–619.

[63] Sircar, S. Pressure swing adsorption. *Industrial & engineering chemistry research 41*, 6 (2002), 1389–1392.

[64] Sjöström, E. *Wood Chemistry: Fundamentals and Applications*. Bibliografía: p. 251-276. Academic Press, 1993.

[65] Staudt, R., Rave, H., and Keller, J. Impedance spectroscopic measurements of pure gas adsorption equilibria on zeolites. *Adsorption 5*, 2 (1999), 159–167.

[66] Stolten, D. *Hydrogen and Fuel Cells: Fundamentals, Technologies and Applications*. John Wiley & Sons, 2010.

[67] Suhas, Carrott, P., and Carrott, M. R. Lignin - from natural adsorbent to activated carbon: A review. *Bioresource Technology 98*, 12 (2007), 2301 – 2312.

[68] Sun, Y., Liu, C., Su, W., Zhou, Y., and Zhou, L. Principles of methane adsorption and natural gas storage. *Adsorption 15*, 2 (2009), 133–137.

[69] Suomen Kaasuyhdistys. Maakaasukäsikirja, 2010.

[70] Teenkrat, D., Hlincik, T., and Prokes, O. *Natural Gas Odorization, Natural Gas*. InTech, 2010.

[71] Thomas, J. M. The existence of endothermic adsorption. *Journal of Chemical Education 38*, 3 (1961), 138.

[72] Tilastokeskus, 2014.

[73] U.S. Environmental Protection Agency. Inventory of U.S. greenhouse gas emissions and sinks: 1990-2012, 2014.

[74] van Erp, T. S., Trinh, T. T., Kjelstrup, S., and Glavatskiy, K. On the relation between the langmuir and thermodynamic flux equations. *Frontiers in Physics 1*, 36 (2014).

[75] Weinberger, B., Darkrim-Lamari, F., and Levesque, D. Capillary condensation and adsorption of binary mixtures. *The Journal of chemical physics 124*, 23 (2006), 234712.

[76] Ye, Y., Ahn, C. C., Witham, C., Fultz, B., Liu, J., Rinzler, A. G., Colbert, D., Smith, K. A., and Smalley, R. E. Hydrogen adsorption and cohesive energy of single-walled carbon nanotubes. *Applied Physics Letters 74*, 16 (1999), 2307–2309.

[77] YLE Uutiset. Tornio saa LNG-terminaalin. `http://yle.fi/uutiset/tornio_saa_lng-terminaalin/7699239`. Posted: 19.12.2014. Accessed: 16.2.2015.

[78] Yu, C.-H., Huang, C.-H., and Tan, C.-S. A review of co2 capture by absorption and adsorption. *Aerosol and Air Quality Research 12*, 5 (2012), 745–769.

[79] Zhou, L. Progress and problems in hydrogen storage methods. *Renewable and Sustainable Energy Reviews 9*, 4 (2005), 395 – 408.